Measuring correlates of perceptual decisions in mouse visual cortex

Christopher P. Burgess

January 2016

Supervisors:

Matteo Carandini

Jennifer F. Linden

Institute of Ophthalmology

Department of Visual Neuroscience

University College London

I, Christopher P. Burgess, confirm that the work presented in this thesis is my own. Where information has been derived from other sources, I confirm that this has been indicated in the thesis.

All that we see or seem is but a dream within a dream.

– Edgar Allan Poe

Abstract

The activity of sensory cortex is determined not only by afferent sensory stimuli, but also by behavioural context factors such as movement, anticipation, attention, and reward. To investigate such factors, I developed a visual psychophysical task in head-fixed mice and combined it with two-photon calcium imaging to measure activity in primary visual cortex (V1).

I trained mice to report the position of a grating by turning a wheel with their forepaws. I found that a crucial element in helping mice learn the task was enabling them to control the position of the stimulus: the grating would initially appear to their left or to their right, and their wheel turns would translate it. They were rewarded for bringing it to the centre.

Mice typically learned the task in 2-3 weeks, producing high-quality psychometric functions of stimulus contrast, with 75% accuracy at contrasts as low as 8%. In the same mice, I injected a virus in V1 to express GCaMP6, so I could perform two-photon calcium imaging of neural populations while the mice performed the task.

Calcium imaging in V1 revealed strong responses evoked by contralateral stimuli, modulated by stimulus contrast. I obtained measures of contrast sensitivity from population responses and found them to be higher than the corresponding psychophysical measures. I did not find significant correlations between perceptual decisions and stimulus-independent V1 activity. I also observed small but significant

increases in calcium activity during pre-stimulus periods and the amplitude of this activity was predictive of subsequent psychophysical performance on those trials.

Finally, I discovered that the basic task was adaptable and the stimulus control principle was generalizable. I demonstrate this by presenting multiple variants of the task including one using auditory stimuli and another probing the effects of dopamine stimulation.

Contents

Table of Figures

Preface

This thesis describes my work developing a perceptual decision-making task for head-fixed mice and my application of it to recording V1 calcium activity in task-engaged mice.

All the work described in this report I performed in the laboratory of my supervisor, Matteo Carandini. The neural recordings described in Chapter 2 were performed in collaboration with Adam Ranson.

In Chapter 1, I describe the approach of using perceptual decision-making tasks in combination with neural recordings to gain an understanding of the neural processes underlying perception, attention and decision-making.

In Chapter 2, I describe my failures and successes in developing a two-alternative forced choice psychophysical task. The chapter describes the results from each of the iterations that the task went through before I arrived at an effective psychophysical task well suited for investigating with neural recordings.

In Chapter 3, I describe the results obtained from two-photon imaging of V1 in mice while they perform the task I developed in Chapter 2. I describe key results from comparisons between neural and psychometric contrast thresholds, finding no stimulus-independent correlates of decisions and observing an unexpected pre-stimulus signal predictive of behaviour.

In Chapter 4, I show examples of how the key elements of the task can be generalised to make variants suited to investigating particular questions.

In Chapter 5, I summarise the key results from the previous chapters a whole, and offer outlook and future directions arising from this work.

Chapter 6 contains appendices describing a selection of supplementary results to the main work.

1 Introduction

As you read these words, your brain is performing an intricate series of computations, effortlessly performing most of the feats that neuroscience is striving to comprehend. Your sensory systems are somehow drawing out a crisp perceptual model of letters and words on the page from an ambiguous and jittering image impinging on your retinas. Regularities in the world have shaped how your brain forms expectations, essential to constraining those ambiguities. Attentional mechanisms bring to bear your brain's limited processing capabilities on the relevant information for the task at hand. Decisions are being made, at multiple levels, from reflexive saccades to motivationally guided choices – like whether to bother reading this text. If we are to have any hope of making sense of these processes, we must study brains which are actively engaged in them. However, the complexity of a seemingly routine task like reading – even if we only consider the perceptual aspects of it – is a reminder that to study these processes, many of the complexities associated with natural behaviours need to be carefully controlled. The study of perceptual decision-making tries to accomplish this by obtaining controlled perceptual measurements and relating them to brain activity. This basic principle is used to study one or more of the processes involved in perception – sensory representation, attention, expectation and decision-making – by asking a brain to discriminate a perceptual feature while measuring or manipulating activity in a region or circuit relevant to that process.

The pioneering work in this field involved combining the assessment of psychophysical performance during a sensory discrimination task with recordings of relevant neural activity (Mountcastle et al., 1990; Newsome et al., 1989a; Vogels and Orban, 1990). These studies compared the sensitivity of behavioural and neural responses (psychometric and neurometric data, respectively) as a function of the stimulus conditions used in the task. They have shown that discrimination ability of single neurons often matches or even exceeds behavioural performance.

Later studies looked at the influence of sensory representations on behavioural choices (Britten et al., 1996; Gold and Shadlen, 2007; Nienborg and Cumming, 2009). This is often expressed in terms of "choice probabilities" (CPs) – the probability that a neural response on a particular trial predicts the animal's choice under a specific stimulus condition. In general, choice probabilities across populations of neurons have been found to be significantly above chance, but modest with respect to single neurons.

The discrepancy between single neuron sensitivity and their CPs suggests that choices are based on the responses of a pool of neurons. This raises questions about what coding is used to represent stimuli across populations, and how this information is used to make decisions. Furthermore, it hints at other non-sensory factors that bias behaviour, such as attention (Raz and Buhle, 2006; Ress et al., 2000), engagement (Otazu et al., 2009), stimulus and reward history (Boneau et al., 1965; Busse et al., 2011).

Nienborg and Cumming, 2009 distinguished these non-sensory factors from sensory ones by considering how the time course of choice correlations, and the effect of reward size should be different if they are sensory or non-sensory in origin. They found that animal performance improved with larger rewards, but choice probabilities were decreased, and that choice-related activity occurred later the influence of stimuli on choices. Consistent with this, Sachidhanandam et al., 2013 showed late choice-related activity in a whisker deflection detection task. They found enhanced depolarisation in the membrane potential of barrel cortex neurons in correct detection trials compared to miss trials. Crucially this choice-modulated depolarisation occurred later than the initial stimulus response.

Other studies have tried to go beyond just choice correlations. For example, Kepecs et al., 2008 found neural correlates of decision confidence in rats performing an odour discrimination task. Houweling and Brecht, 2008 showed that rats could be trained to produce a behavioural report of the stimulation by the experiment of single neurons in barrel cortex. Hanks et al., 2015 was able to relate neural activity to a measure of mentally accumulated evidence derived from the behaviour of rats.

Nonetheless, most studies employing these approaches have been performed in monkey, with single-unit recordings. Increasingly, mice are being used for awake-behaving research due an ever increasing toolkit of powerful techniques for identifying and manipulating particular classes of neurons (Andermann et al., 2010; Huber et al., 2008) and the practicalities of working with them.

Two-photon microscopy enables long-term recordings from large populations of neurons, including the possibility of obtaining recordings from the same set of cells over many weeks (Andermann et al., 2010; Chen et al., 2013; Madisen et al., 2015; Mank et al., 2008). This can be of particular benefit for obtaining recordings from the same cells with a large number of trials and tracking the stability of neurometric data in a defined population over time. Genetically encoded calcium-indicators can be further combined with cell-type specific labelling to probe the role of different neuronal subclasses in perceptual judgements (Bock et al., 2011; Kerlin et al., 2010; Runyan et al., 2010).

Optogenetic techniques enable control over specific subsets of neurons to corroborate causal relationships inferred from the physiology (Cardin et al., 2009; Huber et al., 2008; Luo et al., 2008).

Mouse models have also seen the development of a wide variety of sophisticated behaviours that mice perform head-fixed. This is important because the best neural recordings can be obtained with head-fixed animals because of stability or size constraints of recording probes that restrict portability. Furthermore, for performing psychophysical tasks, head-fixing offers far better control over stimulation. Mice have been trained to perform virtual navigation while head-fixed on spherical treadmills (Dombeck et al., 2010; Harvey et al., 2012; Poort et al., 2015), and to make lever-presses (Histed et al., 2012) and roll trackballs in psychophysical tasks (Kepecs et al., 2008).

The work described in this dissertation was intended to combine the power of the perceptual decision-making paradigm with some of the novel tools available in mouse models just described. I approached this by developing a behavioural task that mice can perform while head-fixed, and I will show that the task enables high quality perceptual measures to be obtained, and is surprisingly flexible. As we shall see, using head-fixed mice allowed me to combine this with two photon calcium imaging of the genetically expressed calcium indicator, GCaMP, for longitudinal imaging. It also enabled the use of optogenetics techniques to perform localised cortical inactivation to demonstrate the dependence of V1 in this sensory discrimination task. However, the full power of this approach has yet to be fully exploited. In particular, one of the promising research avenues that has been opened up is using genetically restricted GCaMP expression to dissect the roles of different cell types in different aspects of perception.

2 A novel perceptual decision-making task for head-fixed mice

In starting this work, I had a number of goals in mind. In particular, I wanted an effective psychophysical task for mice that used simple stimuli, would enable a fine degree of stimulus control and facilitate stable neural recordings. This suggested a head-fixed system.

At the time there were published go/no go task designs for head-fixed mice (Histed et al., 2012) but a two-alternative forced choice (2AFC) design was desirable compared to go/no go designs due to its immunity to variations in criterion and motivation (Carandini and Churchland, 2013). With go/no go designs, a suitable response window must be decided upon, and a baseline go response rate needs to be established to be able to correctly interpret any change in go/no go rate as function of the stimulus. Therefore, if this baseline is variable, for example due to changes in motivation it will confound the estimates of stimulus effect. Furthermore, sensory biases are indistinguishable from changes in the baseline rate. In 2AFC designs, responses are forced, and symmetric. This means guessing always results in 50% performance, and biases and lapse rates can be reliably estimated from psychometric functions (see 2.1). Except for virtual reality systems (Harvey et al., 2012) which use complex stimulation unsuited to classic psychophysical methods, no 2AFC paradigm existed for head-fixed mice.

This led me to develop a technique that enables mice to give reliable reports about stimuli while head-fixed. My initial attempts failed, as mice were unable to learn the simplest task that I started with. However, by adding naturalistically motivated elements I was able to develop a very effective task that I later combined with neural recordings (Chapter 3). In this approach, mice are positioned with their forepaws resting upon a wheel that they can turn with left or right movements. They are trained to perform a task in which their turns are directed by the stimuli. While the task went through a number of iterations, the basic methodology outlined below was used in all the behavioural experiments described in this dissertation.

2.1 General wheel task methods

Head-plate implant

I implanted mice with a metal plate on the cranium to enable their heads to be fixed. To perform this surgery, I injected mice with an anti-inflammatory drug (4 mg/kg carprofen subcutaneously) then anaesthetised them using isoflurane (1–2%). I maintained body temperature at 37°C using a heating pad and protected the eyes with artificial tears to prevent drying (Viscotears). I implanted the head plate chronically, fixing it to the cranium with dental cement (Sun Medical). After surgery, I allowed mice at least 4 days to recover before I began water restriction and behavioural training.

Water restriction schedule

I then placed mice on a water restriction schedule. They were either water restricted for 5 days per week, with access to task reward only, but free access to

water for 2 rest days (no training), or were water restricted continuously with a minimum daily amount (40 µL water per gram, daily mouse weight). The particular schedule used is specified in each task version-specific section below. In either case, I monitored weight, behaviour and general condition, and stopped training and water restriction with any signs of dehydration.

Training procedure

Mice were then trained in a behavioural task, typically in daily one hour sessions over a period of weeks. Before beginning training, mice would be water restricted for two days. On the first two days I only head-fixed and trained naïve mice for ~15 min to reduce stress during acclimatisation. During the first few sessions I typically ran mice on a simplified version of the task, with 100% or 50% contrast, no inter-trial delays, and quiescent or fixed stimulus period. Once they began to start reliably turning the wheel in both directions, I increased these delays to their final values. Once their performance was reliably above chance level, I gradually started to introduce lower contrasts. Typically mice were running on the final task parameters by the beginning or the middle of week 3. Task reward was also usually calibrated throughout the training process. When mice were naïve and did few trials they would be give more per correct trial (~3 µL), and as they became proficient and were completing 300 or more trials they would typically be given ~2 µL.

Task and stimulus control

The task was managed by custom MATLAB software that I developed. The response wheel was a Lego part with a rubber tyre (with a flat 19 mm wide cross stion

and 31 mm in diameter). Its angle was measured using a rotary encoder (in most experiments, a Kübler 05.2400.1122.0100, with resolution: 0.9° or about 0.5mm of wheel circumference) whose signal was acquired using a National Instruments data acquisition device (DAQ). Specific volumes of water were dispensed by opening a solenoid valve (Neptune Research 161T011) for a calibrated duration of time.

Stimuli were presented on an LCD monitor (iiyama ProLite E2273HDS, refresh rate 60 Hz) placed in front of the animal. Monitor luminance values for each colour channel were linearized by using measurements from a photodiode. I used the Psychophysics Toolbox for control of graphics for visual stimulation was MATLAB (Brainard, 1997). The parameters used for Gabor textures were: standard deviations between 5-10°, wavelength 10°, horizontal or vertical orientations.

All experiments were conducted according to the UK Animals Scientific Procedures Act (1986). Male and female C57BL/6J mice between the ages of 8-24 weeks were used for all experiments.

Psychometric analysis

Repeat trials were excluded from psychometric analyses. To compute psychometric functions of contrast, I first calculated the proportion of trials with rightward choices as function of signed stimulus contrast *c*. The sign of *c* indicates stimulus position: positive values denote stimuli on the right; negative values denote stimuli on the left. I fitted these data to the psychometric function (Busse et al., 2011):

$$\psi(c) = \lambda + (1 - 2\lambda)F(c; \mu; \sigma)$$

which here models the probability of rightward choices as a function of contrast. $F(x)$ is the cumulative Gaussian function, parameterised by μ and σ, which determine the bias and slope of the psychometric function. λ represents the lapse rate, which models the fraction of trials that are guessed independently of contrast. I performed the fitting via maximum likelihood estimation using the MATLAB function `fminsearch` over the log likelihood function.

For each training session, the mouse is head-fixed in front of a computer screen with its forepaws resting upon a wheel (Figure 2-1). The mouse can turn the wheel with left or right movements of its forepaws. It can consume droplets of water dispensed via a spout close to its mouth. A nearby speaker can play auditory stimuli.

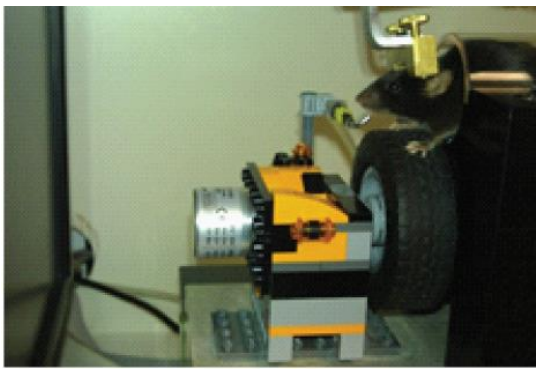

Figure 2-1 Training setup used for wheel tasks.

Mice were head-fixed with their forepaws resting on a wheel, and their body resting in a tube. Visual stimulation was provided on a screen in front of the animal and water spout near their mouth delivered water reward. See main text for details.

The task is organised into successive trials in which stimuli are presented from one of two discernible categories. The mouse is then required to respond with an appropriate wheel turn. The overall turn direction distinguishes it as a left or right

response, one of which is correct for that trial's stimulus category. For correct responses, the mouse receives a water reward (typically 2-3 µL). For incorrect responses, a white noise sound is played during a timeout period.

2.2 Version 1: a simple transient stimulus task

I first attempted to train mice with this technique on a simple task with stimuli presented transiently. I trained them five consecutive days each week during which they only received water as a task reward (typically 0.1-0.9 ml per day, depending on proficiency and motivation). During the two day rests they had free access to water. On each trial, mice were presented with a grating disc (Gabor, see 2.1) for 250-500 ms on the left or the right of the screen together with a low or high frequency pure tone (7 or 12 kHz 200 ms pure tone). The stimuli were consistently paired: the left grating with the low tone; the right grating with the high tone. Mice had 4 s to respond by turning the wheel. Left turns were correct for the left/low stimuli; right turns were correct for the right/high stimuli. Turns after stimulus onset were registered as responses when the speed was above ~40 mm/s. The threshold was optimised by trial and error, informed by typical speeds of small and large wheel turns by mice and choosing it to pick out the faster turns mice were able to make. Missed trials were repeated. Incorrect trials were also repeated to discourage a strategy of turning the wheel in one direction (which would otherwise reap a reward on half of the trials). During the first 2-3 training days, rewards were given for responses in either direction.

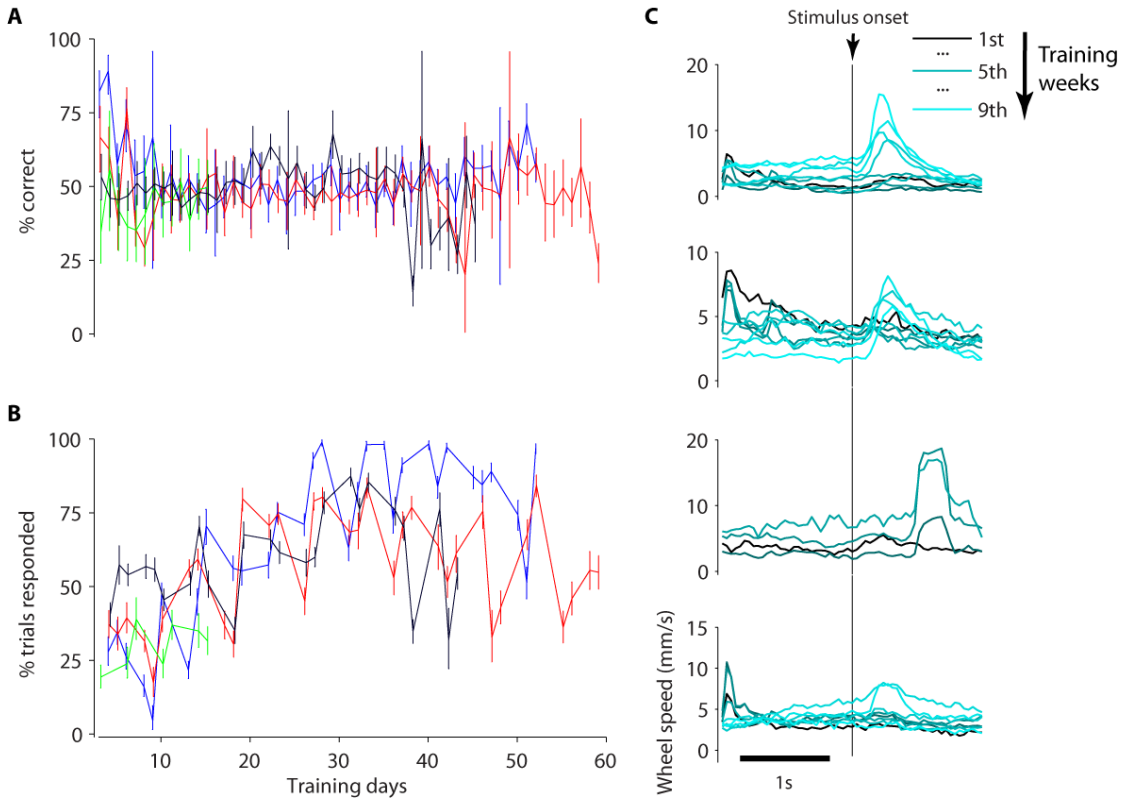

Figure 2-2 Mice failed to learn version 1 of perceptual discrimination task.

A, Percentage correct trials as a function of training day for four mice (different colours). Chance level is 50%. Error bars show 95% binomial proportion confidence interval. The first three training days are not shown as turns in both directions were rewarded. ***B***, Percentage of trials in which mice responded as a function of training day for same mice as in ***A***. The response window is 0-4 s after stimulus onset. Error bars show 95% binomial proportion confidence interval. ***C***, Wheel speed averaged around stimulus onset time over training weeks (graded colours, see legend). Panel rows show the four mice in ***A***.

I implanted four mice then trained them on this task for up to 60 days. Over this period, their responses never surpassed chance-level performance (Figure 2-2A). During latter training weeks, I tested various modifications to make the stimulus more salient (including longer presentation times and making the gratings flicker or drift), but none made a difference to performance. Nonetheless, mice became more

efficient at obtaining rewards as they changed aspects of their behaviour throughout training. Naïve mice quickly learned to turn the wheel, but initially in just one direction. This caused them to become stuck, repeating trials (requiring a counter turn) without rewards. However, over 1-2 training weeks their turn directions became progressively less biased, ultimately enabling them to collect rewards on ~50% of trials. They also learned to initiate their turns after stimulus onset (Figure 2-2C), leading to swifter rewards with fewer turns. This panel also shows that the stimulus-cued response times varied across mice, but did not change with training once acquired. The loss of bias and acquisition of stimulus-cued responses together led to an increase in the fraction of trials with responses over training (Figure 2-2B). These results were encouraging as they showed that mice could competently use a wheel as response device, cued by stimuli. However, they suggested that mice were struggling to relate the direction of their turns to stimulus properties in the task.

2.3 Version 2: using stimulus interactivity to aid learning

In 2.2, mice had failed to associate a stimulus property (in this case visual stimulus position or tone frequency) with their wheel turns. I hypothesised that coupling their actions to changes of the property might help them to form such an association. If they were able to manipulate the property's value along the relevant dimension with their wheel turns then their goal could be to aim the property toward a target value. For example, for visual stimulus position, the stimulus could be presented on the left or the right of the screen as in the previous task, but now the rewarded goal could be to bring the stimulus to the centre, ahead of them. This in

particular, might also benefit from a similarity to natural appetitive behaviour, akin to orienting toward rewarding objects in the environment.

To investigate this rationale as a solution, I developed the following basic design for a new task:

On each trial, a target stimulus is initially presented on the left or the right of the screen. Wheel turns by the mouse translate the stimulus horizontally: left turns move the stimulus to the left; right turns move the stimulus to the right. The mouse's goal is to bring the stimulus to the centre of the screen, whereupon the stimulus locks into place and the mouse receives a reward. If instead the mouse translates the stimulus the same distance in the *wrong* direction, it locks into place there (at the side of the screen) and a white noise sound is played for 2 s to indicate that there is a timeout period. In either case, the stimulus remains locked in its response position for 1-2 s to remind the mouse of its action while it is receiving its feedback, and then disappears.

I applied this basic design in different versions of the task, each with specific stimulus details, timings and conditions. The details of the first version I tested are as follows (also see Figure 2-3).

Methods

Between trials, the screen was black. After trial onset, two grey columns (22° wide, 55° apart), were presented on the left and right of the screen (Figure 2-3B). Next (300 ms later), a horizontal grating (0.1 cycles/°) was superimposed onto one column and all stimuli became movable (*interactive*). The rewarded goal was to get

the grating to the centre. There was no response timeout. The inter-trial interval was 3 s.

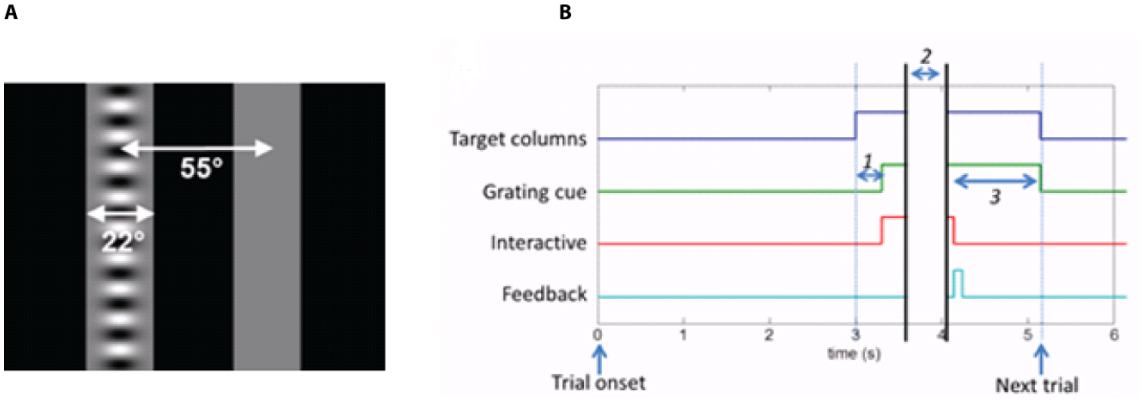

Figure 2-3 A task using visual feedback to aid learning.

A, Visual stimuli used in the first version of ChoiceWorld as seen on the screen (see main text). The stimuli are translated horizontally by the mouse's wheel turns, in the direction of its turns. Stimuli dimensions are indicated by the arrows. ***B***, Temporal sequence of events in the task. *Feedback* is either the delivery of water reward (for correct trials), or the onset of the 2 s white noise sound (for incorrect trials). Refer to main text for more details.

Results

I implanted head-plates in five new mice, and trained them on this task with the same five day training and water restriction schedule as in 2.2 for up to 11 weeks. Mice learned to perform the task with high accuracy (Figure 2-4A). Through the course of each five day water restriction term, mice were increasingly motivated, typically performing few trials on the first water restriction day and the most trials on the last two days (Figure 2-4B, upper panel). Most mice also took longer to complete their responses on Mondays, but there was no effect on other days (Figure 2-4B, lower panel). They were performing above chance by the second or third week so I

gradually introduced lower contrast trials. On the easiest, high contrast trials, proficient mice performed up to 90% of trials correctly, and performed up to 300 trials per day in sessions lasting 30-45 mins.

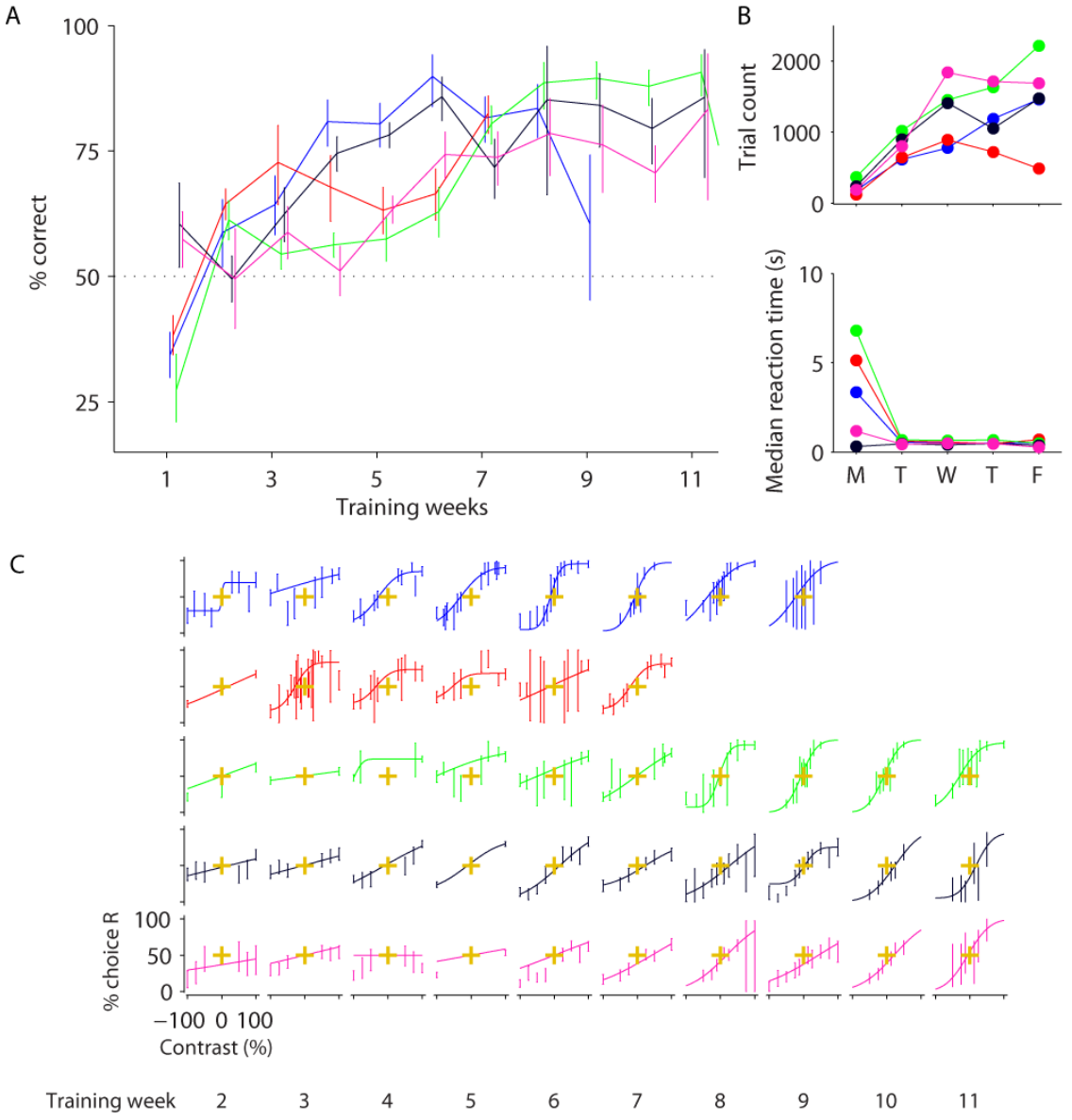

Figure 2-4 Mice learned to correctly report stimuli once visual interaction was introduced (task version 2).

Data from five mice are shown (colour-coded). ***A***, Percentage of correct trials by training week for the easiest trials (the highest contrast trials in each session). Performance was consistently above chance after 3-5 weeks of training. Dashed line indicates chance level. ***B***, Number of trials mice completed, and median reaction time by day of week. Mice were water restricted and trained on weekdays but had free access to water at weekends. ***C***, Psychometric functions for contrast by week (panel columns). The proportion of trials that the mouse chose the right-hand grating (choice R) is plotted as a function of the signed grating contrast, where the sign represents grating position (negative for left-hand side, positive for right-hand side). Task was as described in the main text and Figure 2-3. All error bars show 95% binomial proportion confidence interval.

I analysed their choices as function of stimulus contrast and fitted psychometric functions to the data. The functions are determined by three parameters: lapse rate, contrast bias, and contrast threshold. The parameters each pertain to different aspects of animal choices. The lapse rate reflects the proportion of trials with choices made independent of the stimulus. The contrast bias denotes the contrast at which choices are balanced, i.e. 50% to the left and right. The contrast threshold reflects contrast sensitivity: the lower the threshold, the sharper the modulation of choices by contrast.

I obtained psychometric functions across training weeks to chart learning (Figure 2-4C). As training progressed, psychometric functions stabilised, eventually producing consistent contrast thresholds, and small biases in later weeks. I pooled data across these weeks for more detailed behavioural analysis (Figure 2-5). In the psychometric analyses (Figure 2-5A), the psychometric functions are plotted along with their parameters. Three mice have similar contrast thresholds (~35%; top three panels, Figure 2-5A) but the other two have relatively high thresholds (> 50%).

Reaction times were largely distributed between 0.1-1 s (Figure 2-5B) but with a long tail ranging up to 40 s due to not enforcing a response time limit. In 3/5 mice, there was a trend for slower reactions on the lowest contrast trials (top three panels in Figure 2-5C). Furthermore, in those mice, the slowest reaction times tended to follow the contrast bias (obtained from the psychometric functions).

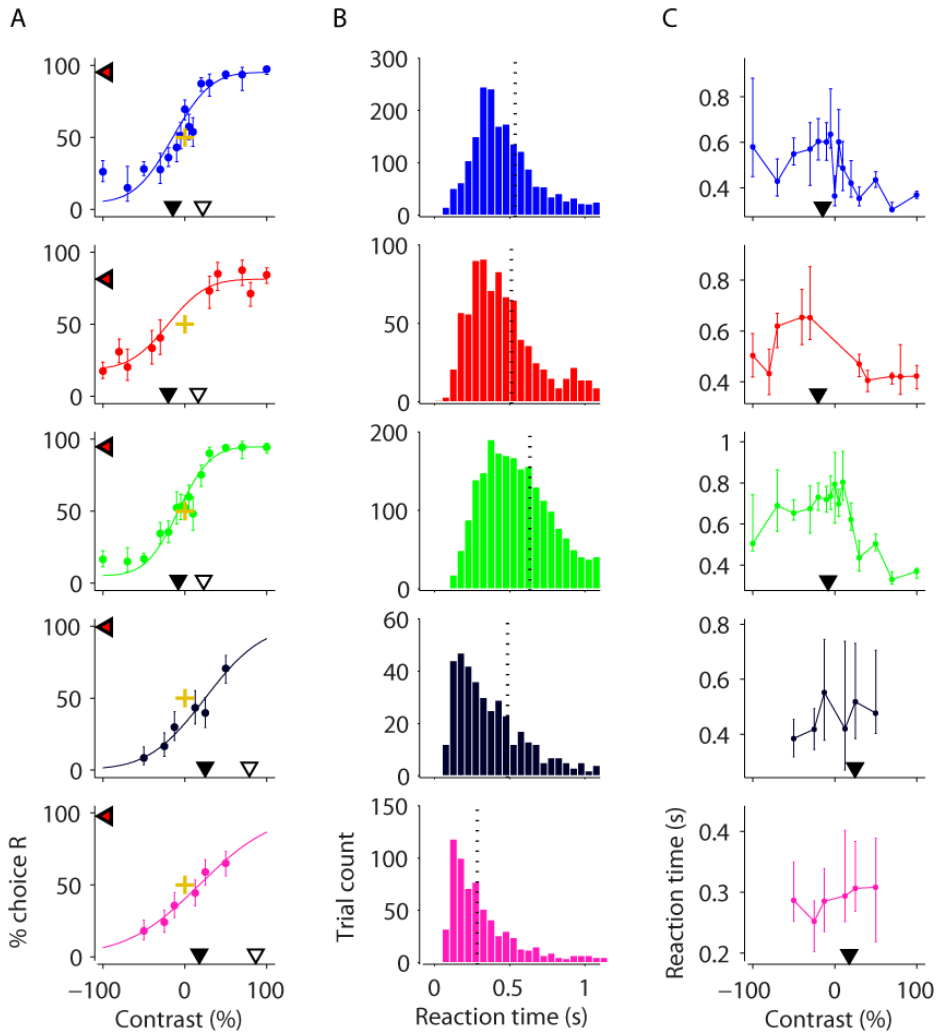

Figure 2-5 Behavioural analysis of data from proficient mice in task version 2.

Pooled analyses of last 1-3 training weeks (with stable performance) of mice in Figure 2-1. ***A***, Contrast psychometric functions. Filled black triangles indicate the contrast bias (the contrast at which the mouse chose the left and right equally). Difference in contrast between open and filled black trials indicates the contrast threshold. Red/black triangles indicate the lapse rate (proportion of guessed trials) by their decrement below 100% choice R. Gold crosses show 0% stimulus contrast and 50% choice intersection point for reference. Error bars show 95% binomial proportion confidence intervals. ***B***, Reaction time distribution (time to reach the wheel turn response threshold from grating onset). Vertical dashed line indicates median reaction time. ***C***, Reaction time as a function of grating contrast and position. Data points indicate medians and error bars show 40th and 60th percentiles. Contrast biases from ***A*** are shown for reference (filled black triangles).

These results support the hypothesis that enabling mice to interactively move the stimulus with the wheel helped them learn to direct their turns according to stimulus position.

Task refinements

From a purely behavioural perspective, the new task was successful in that mice were able to learn it and to generate high quality psychometric data. However, for relating stimuli and behaviour to visual neural responses, the task design presented a number of issues.

One issue was the complexity of the visual stimulation: a number of stimulus attributes changed close together in time. There was stimulation both from the target grating and the grey columns. Furthermore, the appearance of grey columns on a black screen caused a large change in overall mean luminance, which is known to invoke retinal adaptation (Barlow and Levick, 1969) and affect psychophysical contrast thresholds (Kilpeläinen et al., 2011). Separating out these factors in neural responses would present additional challenges, particularly with calcium imaging, which has a relatively low temporal resolution (e.g. GCaMP6m transients are reported to peak after ~0.1 s and half-decay in ~0.4 s, Chen et al., 2013). Interpreting neural responses would be more straightforward if the only stimulus change was the appearance of the target itself.

More problematically, the presentation of the target stimulus was poorly controlled. Mice were able to start moving the target as soon as it appeared. Firstly, this complicates comparison between trials, as each stimulus trajectory is controlled

by the mouse. Moreover, any attempt to study the relationship between choice and neural activity is confounded by the introduction of a direct correlation between choice and stimulus movement. One solution to both these issues could be to only analyse trials where the turn (and therefore the stimulus movement) starts late. However, this might introduce other unintended confounds by selecting atypical trials, which might e.g. be those with lower contrasts or where the mouse is satiated. In practice this would also severely limit the number of trials available for analysis, again because proficient mice initiate their responses swiftly (see Figure 2-5B). If however, the target stimulus was made unmovable for a brief period at presentation, neural responses would be controlled in that window.

Finally, there was a fixed delay between the offset of one stimulus and the onset of the next. With a recording technique that uses with low resolutions such as GCaMP calcium imaging, a fixed delay could make it difficult to disambiguate offset and onset responses to visual stimuli. A randomised interval would solve this problem.

2.4 Version 3: controlled stimuli

To address these issues, I developed a new version of the task. To eliminate the mean luminance change and reduce stimulus complexity, the screen background was made grey and the grey columns were abolished. In this version, the target grating was the only stimulus presented. Previously, the grey columns had acted as a cue for the mouse to make a choice. To replace that, I added a tone, presented 500ms before target onset. To better control stimulus presentation, the target was

held in its initial position and did not become interactive until 1 s after onset. To help separate offset and onset responses, a random inter-stimulus interval was introduced, picked on each trial from a uniform distribution between 2-5 s.

Results

I implanted two new mice and trained them on this version. These mice were trained and water restricted seven days a week, receiving a minimum daily amount by topping up any deficit from task rewards (see 2.1). In collaboration with Adam Ranson, we also implanted and trained another three mice and performed two-photon calcium imaging on them. However, due to technical issues with the recordings (including degradation in indicator expression and cell health, see 6.3) the imaging data are not presented in this thesis. Details of the two-photon calcium imaging methods and results from other experiments can be found in Chapter 3.

I started the training with high contrast trials, and short inter-stimulus (1 s) and interactive intervals (0-0.5 s). As training progressed these were increased to their final durations (more details can be found in 2.1).

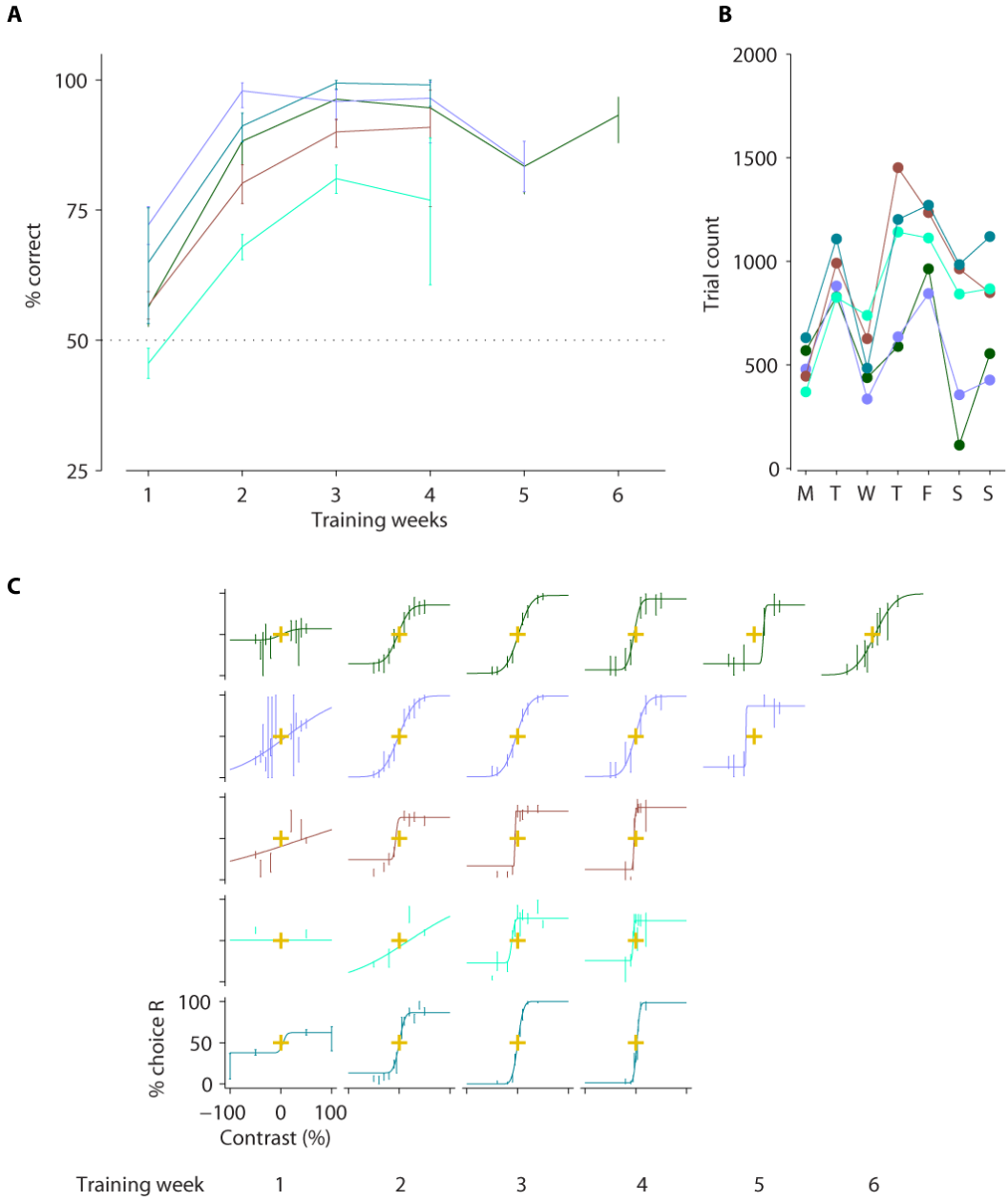

Figure 2-6 Rapid acquisition of task version 3.

Data from five mice are shown (colour-coded). ***A***, Percentage of correct trials by training week for the easiest trials (the highest contrast trials in each session). Performance was consistently above chance by the second week of training. Dashed line indicates chance level. ***B***, Number of trials mice completed by day of week. Mice were water restricted and trained seven days a week without free water breaks. ***C***, Psychometric functions for contrast by week (panel columns). The proportion of trials that the mouse chose the right-hand grating (choice R) is plotted as a function of the signed grating contrast, where the sign represents grating position (negative for left-hand side, positive for right-hand side). Task was as described in the main text. All error bars show 95% binomial proportion confidence interval.

Mice learned to perform this task proficiently after 2 weeks of training (Figure 2-6A). For some mice, performance on the easiest trials dropped in later weeks of training after being given a particularly large proportion of difficult (low contrast) trials. With the continuous training schedule there was no trend by training day for motivation (Figure 2-6B). High-quality contrast psychometric functions were typically produced from the second week onwards, and were stable across weeks (Figure 2-6C), producing psychometric curves with little bias and similar contrast thresholds. As with the previous version, I performed a detailed behavioural analysis of data pooled data across these the weeks (Figure 2-7). The psychometric analyses revealed generally lower contrast thresholds and biases than in the previous task (Figure 2-7A vs Figure 2-5A, and also see the summaries in Figure 2-9). As in the previous version, reaction times were generally slower for more difficult trials (i.e. lower contrast).

This cohort learned faster and performance was more reliable sooner than those in the previous task version (Figure 2-6A vs Figure 2-4A). Although I did not investigate this further, this could be for a number of reasons including more careful training, the improved training and water schedule (supported by stabilised motivation, Figure 2-6B) and also the simpler stimulus (since mice were only presented with one stimulus in this version, they did not need to learn which was the important one).

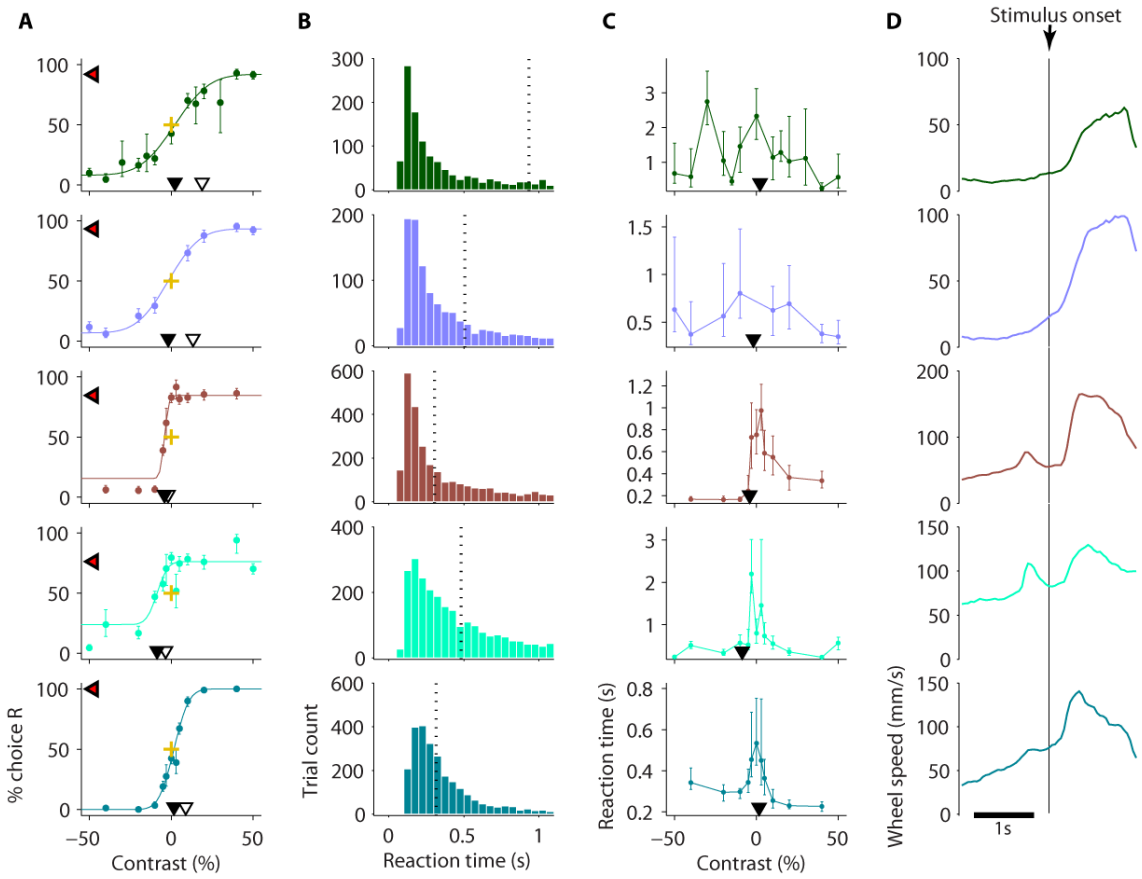

Figure 2-7 Behavioural analysis from mice proficient in version 3 of the task.

Pooled analyses of all sessions from the third week of training onwards of mice in Figure 2-6. ***A***, Contrast psychometric functions. Filled black triangles indicate the contrast bias (the contrast at which the mouse chose the left and right equally). Difference in contrast between open and filled black trials indicates the contrast threshold. Red/black triangles indicate the lapse rate (proportion of guessed trials) by their decrement below 100% choice R. Gold crosses show 0% stimulus contrast and 50% choice intersection point for reference. Error bars show 95% binomial proportion confidence intervals. ***B***, Reaction time distribution (time to reach the wheel turn response threshold from *interactive*, 1 s after grating onset). Vertical dashed line indicates median reaction time. ***C***, Reaction time as a function of grating contrast and position. Data points indicate medians and error bars show 40th and 60th percentiles. Contrast biases from ***A*** are shown for reference (filled black triangles). ***D***, Wheel speed averaged around stimulus onset time.

The modifications now meant a single stimulus change on each trial, a period with controlled stimulus position, and a randomised separation between stimulus

offsets and onsets. After obtaining these results, I became more confident that the general principles that informed the design of the task were actually responsible for the good performance in the task and that specific details could be changed without adversely affecting performance.

2.5 Version 4: controlling wheel movements

I had two more potential concerns with measuring neural activity during the task that I wanted to address. One concern was the issue of uncontrolled movements of the mouse before stimulus onset. It is known that neural responses in V1 are affected by running (Ayaz et al., 2013; Keller et al., 2012; Saleem et al., 2013). If the effects of wheel movements are similar it may complicate interpretation of responses: in 2.4, mice tended to be making significant wheel movements in the period leading up to stimulus presentation (Figure 2-7D). The other concern was that the vertical extent of the stimulus (65°) would evoke responses over large strip of V1. I hypothesised that, given a fixed pool of neurons that can be recorded, the more neurons that carry information about the stimulus, the less likely it is that the recorded ones will be carrying a significant proportion of the information guiding further processing and decision-making. Thus, it may be preferable restrict the size of the target stimulus.

To address these concerns, I made the following modifications. To control for wheel movement at stimulus onset, I introduced a 2-3 s *quiescence* period: a random duration was picked for each trial uniformly from 2-3 s, and each stimulus was not presented until mice had not moved the wheel for the full duration. To shrink the

population of neurons that respond to the stimulus, I used a circular Gabor grating (standard deviation 7.5°; ~18° full width half maximum) instead of the grating column. This size ensured that at least grating two cycles of the grating were visible when presented at 0.1 cyc/° (this spatial frequency is approximately the peak of mouse contrast sensitivity, Histed et al., 2012). In this version, the onset tone was presented 100 ms before the visual stimulus.

Results

I trained three new mice on this version and learning proceeded at a similar rate to the previous task (Figure 2-8A) with proficient mice performing the easiest trials at ~90% accuracy. Their psychometric functions had stabilised by the third week of training and produced high quality psychometric curves (Figure 2-8B).

A detailed analysis of data obtained from the third week onwards (Figure 2-8) showed similar contrast thresholds and biases to the previous version (Figure 2-8C vs Figure 2-7A, and summaries in Figure 2-9). Contrast thresholds were slightly increased, presumably due to the stimulus being smaller. Median reaction times were slower, but the fastest reaction times were quicker (Figure 2-8E vs Figure 2-7B), possibly because of the state of readiness facilitated by the enforced quiescent period before stimuli. Possibly related to this, reaction times showed a much clearer trend for slower times with decreasing contrast (Figure 2-8E).

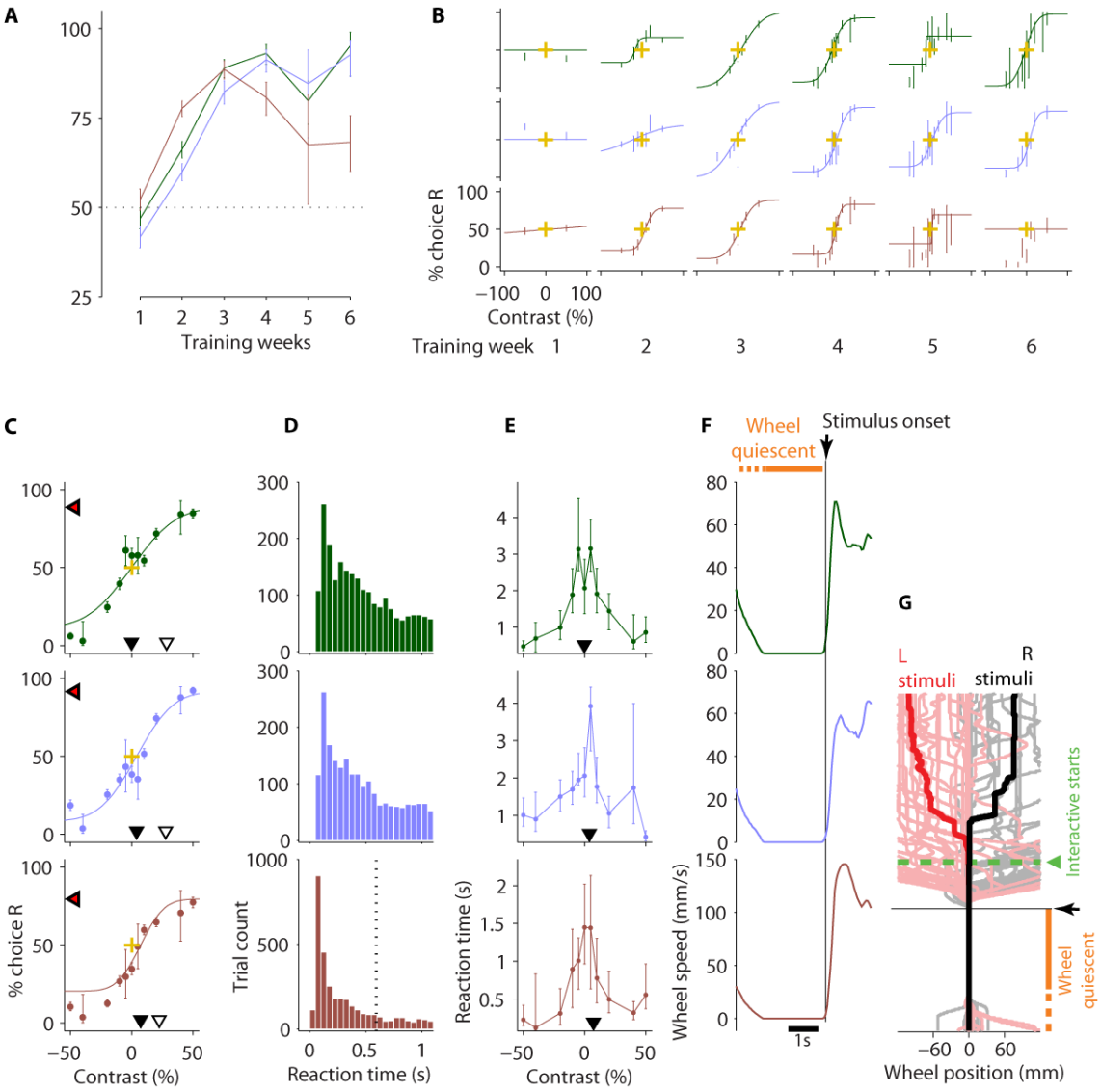

Figure 2-8 Task acquisition and stable psychometrics in version 4.

Data from three mice are shown (colour-coded). ***A***, Percentage of correct trials by training week for the easiest trials (the highest contrast trials in each session). Dashed line indicates chance level. ***B***, Psychometric functions for contrast by training week (panel columns). ***C***-***F***, Pooled analyses of sessions from the third week onwards. ***C***, Contrast psychometric functions. Filled black triangles indicate the contrast bias (the contrast at which the mouse chose the left and right equally). Difference in contrast between open and filled black trials indicates the contrast threshold. Red/black triangles indicate the lapse rate (proportion of guessed trials) by their decrement below 100% choice R. Gold crosses show 0% stimulus contrast and 50% choice intersection point for reference. Error bars in ***A***-***C*** show 95% binomial proportion confidence intervals. ***D***, Reaction time distribution (time to reach the wheel turn response threshold from *interactive*, 1 s after grating onset). Vertical dashed line indicates median reaction time (out of bounds in top two panels). ***E***,

Reaction time as a function of grating contrast and position. Data points indicate medians and error bars show 40th and 60th percentiles. Contrast biases from ***C*** are shown for reference (filled black triangles). ***F***, Wheel speed averaged around stimulus onset time. ***G***, Wheel trajectories relative to stimulus onset time (black arrow and horizontal line) grouped by stimulus position (red for left stimuli; black for right stimuli). Two thick traces show median position, thin traces show individual trials. Green line and arrow indicates time stimulus became movable (*interactive*). 2-3 s pre-stimulus *quiescence* period (requisite wheel stillness before stimulus presentation) indicated by orange bars in ***F***-***G***.

This data showed that the stimulus change (to a circular Gabor grating) and the imposition of the pre-stimulus quiescence period did not impact learning acquisition or overall performance. Moreover, the quiescence period was now prominently displayed by the complete lack of wheel movement leading up to stimulus onset in the wheel trajectories (Figure 2-8F vs Figure 2-7D). This is highlighted in a plot of individual and median wheel trajectories relative to stimulus onset time grouped according to stimulus position (Figure 2-8G). This plot also shows that mice in this task did not tend to wait for the stimulus to become interactive (green line 1s after stimulus onset) before initiating their responses.

In collaboration with Adam Ranson, these mice were also injected with GCaMP6m virus, and imaged while they performed the task. The imaging results are discussed further in Chapter 3.

Finally, to enable comparison of psychophysical performance obtained across the different tasks (and with other studies), I compiled summary statistics of the psychometric function parameters across all the animals trained in task version 2-4 (Figure 2-9). Contrast thresholds were considerably higher in version 2, presumably

because of the presence of other stimulus changes which the mice had to ignore, including a large mean luminance change at stimulus onset, which will invoke adaptation. Biases were smaller and more consistent in task versions 3 and 4. Thresholds were generally higher for task version 4, possibly because the stimulus is smaller than in task version 4 (and the narrow grating column used in version 3 is unlikely to invoke considerable surround suppression) although more data would be needed to support this conclusion.

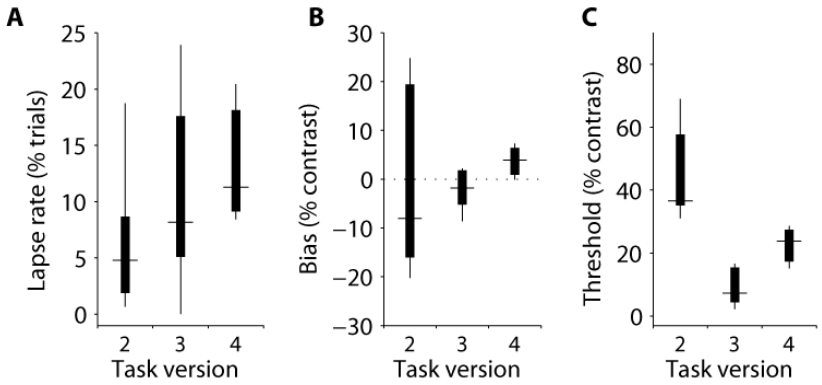

Figure 2-9 Psychometric parameters across task versions.

Summary of parameters from model fits to contrast psychometric data of all mice by task version. ***A***, Lapse rates (percentage of trials in which the stimulus is ignored and the mouse guesses). ***B***, Contrast bias (the contrast at which the mouse made an equal proportion of left and right choices). ***C***, Contrast threshold (the contrast increment required to go from equal choices to ~84% of the upper bound in right-hand stimulus choices; upper bound is 100% minus the lapse rate). Data are summarised in box plots: horizontal bars are medians, box edges are 25th and 75th percentiles and the ends delineate the full ranges.

2.6 Discussion

I have described the development of an effective two-alternative forced choice task for head-fixed mice. First, I showed that mice were not able to learn the task under a simpler regime where stimulus properties were unconnected to wheel movements except via subsequent reward. Second, I showed that after giving mice control of stimulus position with the wheel they were able to make visually guided choices and produce high quality psychometric data. Third, I developed the task through a number of iterations that were motivated by improving the interpretation of planned neural recordings during the task. In spite of these changes, behavioural performance remained robust across all iterations.

So why did mice not learn the simple task, but did learn when they were given control over the stimulus? I would speculate that mice lacked the cognitive abilities to form an abstract link between the positions of fixed gratings and the directions of their wheel turns, especially given that the link itself is only reinforced once per trial via operant conditioning. In contrast, in the interactive task, mice receive continuous feedback about their actions with the wheel, which may help form the required link. Furthermore, they can use the wheel to move the stimulus through a continuous space, which may appeal to natural egocentric orienting and grasping behaviours, and their underlying brain mechanisms (Glimcher, 2003; Gnadt and Andersen, 1988; Scherberger and Andersen, 2007).

This is particularly true given that mice had to turn the wheel in the direction they wanted the stimulus to move – forces of the same direction would produce the

same effect in the real world: e.g. to move toward an entity off to the left you apply force to toward the right on the ground to move yourself left, *or,* to bring an entity on your left toward your fore, you should apply a force its right. Furthermore, the mice were rewarded for bringing an initially distal stimulus to their fore, which is an appetitive-like behaviour.

A variety of different sensory guided tasks have been developed for mice, each with their own subset of features and ideal applications. This includes a freely moving two-alternative forced choice paradigm (Busse et al., 2011), and head-fixed go/no go style designs, either in virtual reality (Poort et al., 2015) or with simple, controlled stimulus presentation (Glickfeld et al., 2013; Histed et al., 2012). This task offers a head-fixed two-alternative forced choice (2AFC) paradigm with simple stimuli (and mostly controlled, particularly as the interactivity restricted in time) and relatively rapid learning, making it ideally suited to psychophysical investigation. Sanders and Kepecs, 2012 have published a 2AFC task for head-fixed mice suited to auditory psychophysical measurements, which also uses a wheel-like device controlled the mouse's forepaws for getting reports.

On its own, this is an effective task for performing head-fixed psychophysical experiments in mice. However, by providing a rigorous a psychophysical measure to relate to neural activity, combining it with neural recordings in sensory cortex makes it possible to investigate sensory contributions to perception. In the next chapter we shall look at V1 activity while mice perform the final variant of the task (version 4).

3 V1 calcium activity during behaviour

3.1 Introduction

My goal was to be able to obtain rigorous psychophysical measurements from mice for comparison with simultaneously measured sensory activity. In the previous chapter, I demonstrated an appropriate task for this purpose, but what is the most suitable recording method? There are two factors stand out as particularly relevant to recordings during perceptual decision-making. One is the value of obtaining significant amounts of data from large populations of the same cells. Analysing patterns of correlations among different sources of variability is a common feature of many of the analysis techniques used in the study of perceptual decision-making. This usually requires a lot of trials or data in general. Another factor is the value of the trained animal. While required training periods are relatively short in the task (especially compared to primates), training mice still requires some time and their performance can be variable across sessions, especially if distressed. This means acute methods are often risky and can be low yield.

GCaMP calcium imaging uniquely addresses these requirements by enabling imaging of the same cells over a period of weeks or more (Chen et al., 2013; Madisen et al., 2015). I chose to use calcium imaging for these reasons. However, it is also important to be aware of, perhaps, its chief limitation: temporal resolution. This significantly improved with the availability of the GCaMP6 family (Chen et al., 2013). However, for certain questions electrical recordings are still the best method,

particularly those concerning temporal aspects of sensory coding or the timing of information flows during perceptual decisions.

I collaborated with Adam Ranson to perform two-photon calcium imaging of V1 in mice engaged in the task.

3.2 Methods

I performed behavioural methods including, water restriction schedule, training procedure, stimulus delivery and psychometric analysis as described in 2.1. Specifically task version 4 (see 2.5) was used in all experiments described in this chapter.

Intrinsic signal mapping of retinotopy

To ensure expression of GCaMP in a V1 region with receptive fields covering the onset position of the task stimulus, we obtained stereotaxic coordinates for virus injections using intrinsic signal mapping (Grinvald et al., 1986) in two mice. We anaesthetised the mice with isoflurane and presented them with drifting gratings while the right cortex was illuminated with green light (530±20 nm; Thorlabs LED) and imaged (PCO camera) at 10 Hz. The gratings were randomly centred at one of three different azimuths along the horizontal meridian in the left visual hemi-field. We computed mean haemodynamic response maps to stimuli in each position from the imaging frames. We measured the stereotaxic coordinates at the centre of the V1 response patch (blue arrowhead in Figure 3-1A) to the middle grating, which corresponded to the onset position of the left target stimulus used during training.

We obtained mean stereotaxic coordinates of 2.8 mm lateral and 3.3 mm caudal to bregma (right hemisphere).

Expressing GCaMP in V1 neurons

We anaesthetised three 10-12 week old C57BL/6J female mice with isoflurane and implanted them with a metal head plate attached to the skull. We performed a 1mm^2 craniotomy in the middle of a circular aperture in the head plate. The craniotomy was centred in the right cortex at the stereotaxic coordinates obtained from the intrinsic signal mapping experiment (see above). We then injected them with GCaMP6m virus (AAV2/1-*syn*-GCaMP6m-WPRE, adeno-associated virus with human synapsin promoter driving expression of GCaMP6m, undiluted 2x10^{13} genome copy/ml from Penn Vector Core; Chen et al., 2013) into the centre of the craniotomy at a depth of 250 µm beneath the dura. We then covered the craniotomy with a two-layer glass coverslip construction, and sealed it with dental cement. The mice were allowed to recover for 1 week before water restriction and head-fixed training began. Water restriction was on a continuous schedule (see 2.1).

I trained the mice in task version 4 (described in 2.5), a Gabor discrimination task (trial structure is illustrated in Figure 3-2B).

Measuring V1 calcium activity during task performance

I began calcium imaging 3 weeks after virus injection. Imaging was performed using a Sutter two-photon movable objective microscope controlled by ScanImage (Pologruto et al., 2003). A Coherent Chameleon laser running at 1000 nm provided excitation, with power level controlled by a Conoptics pockels cell. Images were

acquired continuously at 12Hz with a resolution of 128×128 pixels. An Olympus 20X object was used for focusing. Imaging data was synchronised with behavioural and stimulus events by simultaneously acquiring signals with imaging frame events and screen refresh events (using a photodiode directly measuring the screen).

In each mouse, I chose a field of view with good GCaMP expression for longitudinal behavioural imaging. I mapped the preferred stimulus position of the field of view by imaging the field of view while repeatedly presenting a grating stimulus on a grey screen (same as in the task) for 1 s with 1-2 s inter-stimulus intervals. Stimuli were presented at positions drawn randomly from a 5×5 grid in the left hemi-field. The mean stimulus response across the field of view was calculated at each stimulus position. The position evoking the largest response was taken as the field of view's position preference.

I installed the behavioural apparatus under the microscope (illustrated in Figure 3-2A) and imaged the mice while they performed the task. Before behavioural imaging commenced, I shifted the task stimulus onset position to the preferred position of the chosen field of view (the shift was typically < 10°).

Data analysis

I first registered the raw calcium movies using an algorithm that aligns each frame to the peak cross-correlation with a reference frame using the discrete Fourier transform (Guizar-Sicairos et al., 2008). I found cell regions of interest (ROIs) either by hand or by using a semi-automated algorithm that finds nearby pixels that are significantly correlated with each other. Δ*F/F* calcium signals of ROI traces were

computed as in Jia et al., 2011. Briefly, from calcium traces *F*, I obtained a measure of baseline F_0 by smoothing *F* in time (0.75s causal moving average) and finding the minimum over a (causal) sliding window (20s). Δ*F/F* is computed by computed by applying a causal exponentially weighted filter (τ = 0.2 s) to the fractional change $(F-F_0)/F$. In trial-based analyses, I did not use data from repeat trials (trials repeated due to an incorrect choice by the mouse).

For neural decoding I trained support vector machines (SVMs; Cortes and Vapnik, 1995) on vectors of neural activity to linearly classify the stimulus position or choice of trials. I trained and tested classifiers using the `svmtrain` and `svmclassify` MATLAB functions, respectively, in the Statistics Toolbox.

I fitted intervals to bouts of wheel turns in the wheel speed trace using a Schmitt trigger-based dynamic threshold procedure. I adjusted the two thresholds by hand until they appeared to produce good fits the bouts.

I computed movement onset- and offset-triggered average calcium activity from segments of cell Δ*F/F* traces around the onset or offset events. For each cell I averaged across these Δ*F/F* segments but I excluded any periods with a stimulus present and until 3 sec after stimulus offset from these averages.

3.3 Results

GCaMP expression in task-stimulus responsive V1 neurons

We performed virus injections in three mice to express GCaMP6 and implanted a chronic imaging window over the area (Figure 2-1A). I then trained the

mice in the *Gabor* position discrimination task (Figure 3-2B; task version 4 described in 2.5). Once their GCaMP expression was bright and they had achieved stable psychometric performance (after two weeks of training, see Figure 2-8) they were used for two-photon imaging. A field of view was chosen (100x100 μm; Figure 3-1C) and its overall receptive field preference was measured (Figure 3-1D). The preference was used to fine-tune the onset position of the target stimulus to maximise responses in the field of view. I was then able to return to the same field of view over multiple imaging sessions in mice while they performed the task (setup shown in Figure 3-2A).

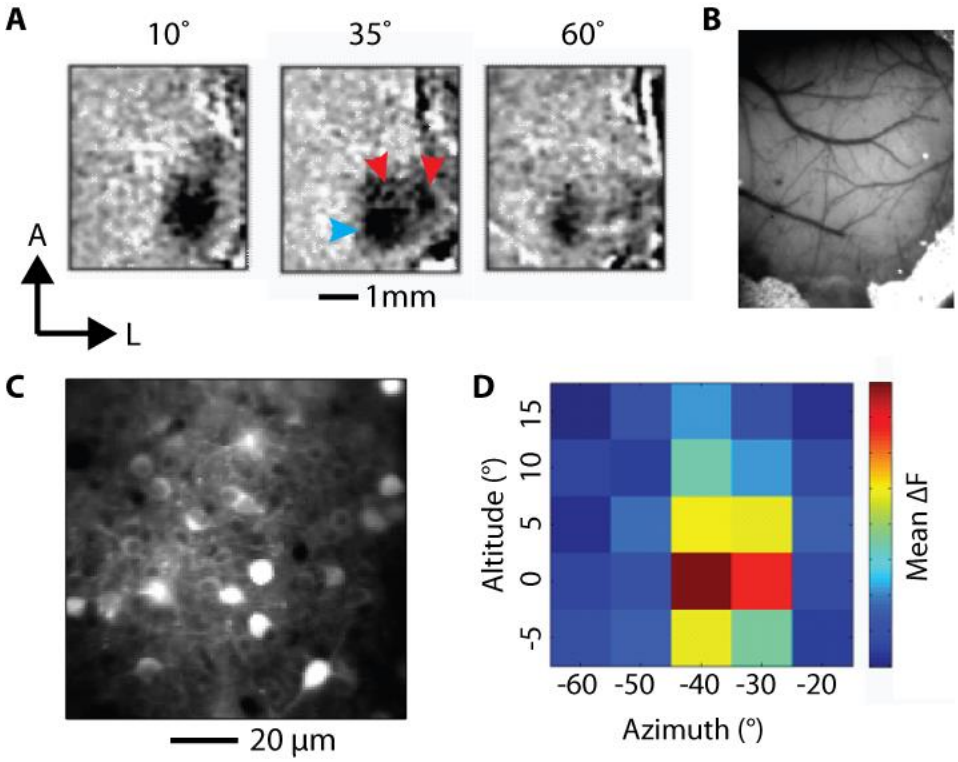

Figure 3-1 Targeted expression of GCaMP in V1 neurons

A, Intrinsic signal maps used to obtain stereotaxic coordinates for virus injection. Mean responses to stimuli at different positions. Stereotaxic coordinates were obtained from the V1 response patch (blue arrow) was distinguishable from responses in higher visual areas (red arrows). ***B***, Imaging window over V1. ***C***, Example field of view from two-photon calcium imaging chosen for longitudinal imaging. ***D***, Results from retinotopic mapping of the field of view in ***C***. The same Gabor grating used in the task was repeatedly presented in multiple locations. The peak response location was used to position the grating stimulus in the task.

Responses modulated by position and contrast

I typically identified 20-30 cell regions of interest (ROIs) in a given field of view. Among those I found cells with clear calcium transients evoked in response to the contralateral target stimulus (Figure 3-2C).

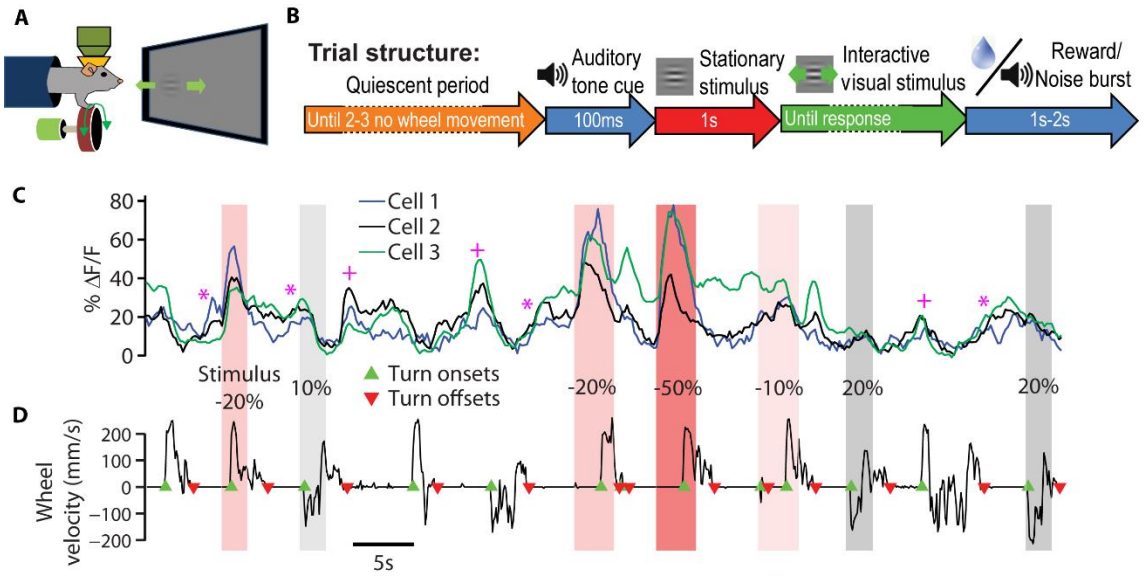

Figure 3-2 Imaging V1 calcium activity during behavioural task performance

A, Schematic of imaging and behavioural setup. ***B***, Trial structure of the task. The task used was version 4 described in 2.5. ***C***-***D***, Calcium activity from three example cell regions of interest (***A***) and wheel turn velocity (***B***) over time during a typical behavioural recording session. Shaded regions indicate periods with stimuli present and their type (red shading indicate contralateral stimuli, grey shading indicate ipsilateral stimuli; shading intensity and text indicates contrast level). Turn onsets (green triangles) and offsets (red triangles) from a fitting procedure (see main text) are shown on the wheel velocity plot. Magenta asterisks show examples of pre-stimulus activity build-ups; magenta crosses show examples of build-ups in longer intervals between stimuli.

To assess the modulation of V1 cells by task stimuli, I computed trial averages of cell traces (cell ROIs in Figure 3-3A) around grating onset time. These showed a rapid rise in fluorescence following the onset of contralateral stimuli (Figure 3-3B). Responses were at or close to the peak by the time the stimulus became movable (*interactive*) after 1 s. In contrast, fluorescence typically decayed after ipsilateral stimuli or on blank trials. I found that response amplitude increased with the contrast of contralateral stimuli but was unmodulated by ipsilateral stimulus contrast (Figure

3-3C). The difference in Δ*F*/*F* amplitude for the strongest stimuli and blanks ranged between 7-50% (mean 18%±16%).

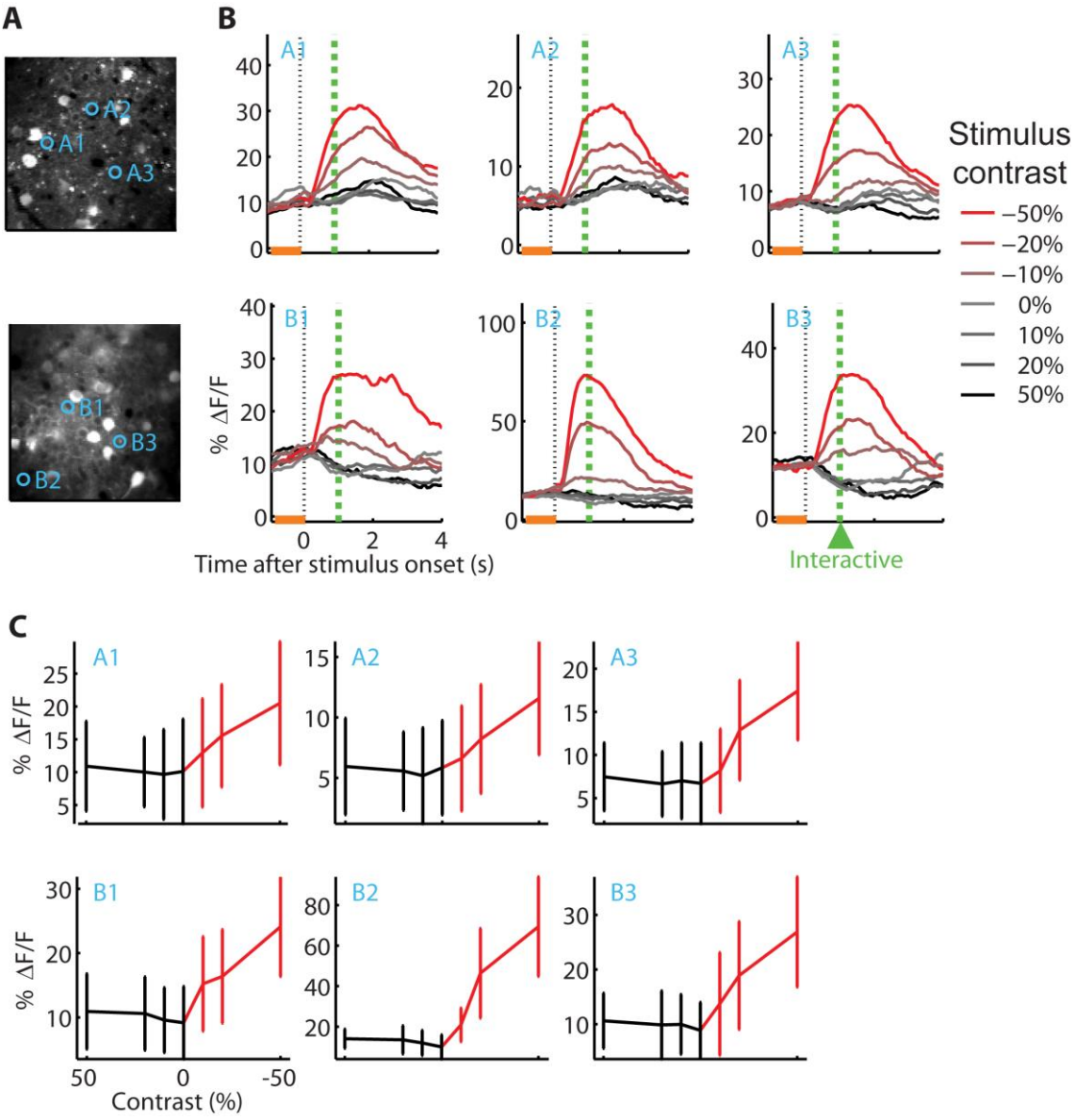

Figure 3-3 V1 calcium responses modulated by stimulus position and contrast

Calcium activity in response to contralateral (red traces) and ipsilateral (black traces) stimuli presented during behavioural experiments in two mice (row-wise). ***A***, Imaging field of view (showing mean calcium fluorescence across a session), each with three cells delineated (labelled blue circles). ***B***, Mean calcium activity averaged around the onset of the grating stimulus, grouped by stimulus condition (colour-coded lines, see legend) for the three cells (panel columns, blue cell label inset). Orange bar shows part of the period of no wheel movement required before stimuli are presented. Dashed green *interactive* line indicates the moment the stimulus becomes movable. ***C***, Response amplitudes of each cell to different stimulus contrasts and positions. Amplitude is mean response at 1 s after grating onset. The x-axis is reversed to emphasise that response amplitudes increase with contralateral stimulus contrast.

Decoding task and behavioural variables

Given that both mouse choices and sensory responses were dependent on stimulus position, I was able to ask how they related to one another. In order to compare stimulus coding with psychometric assessments, I measured the reliability of stimulus position decoding from population activity as a function of contrast. To do this, I trained support vector machines (SVMs) to classify stimulus position using pixel vectors of the stimulus response movies (Figure 3-4A). The SVMs were trained on half the trials of a single session, then tested on other unseen trials from the same session or subsequent sessions. I then counted classifications as a function of contrast and position and fitted this data in the same way as with psychometric data (0) to obtain neurometric functions (Figure 3-4B). Compared with the corresponding psychometric functions obtained from mouse choices on the same trials (also in Figure 3-4B), neurometric functions were steeper, indicating higher contrast sensitivity. This suggests mouse choices were not based on all the information available in a just a single imaging field of view. Due to the classifier being trained on neural responses from a single hemisphere, the neurometric functions were more biased than mouse choices (see 6.4 for explanation), and consistently to the left (i.e. the contralateral side; see response bias in Figure 3-3C).

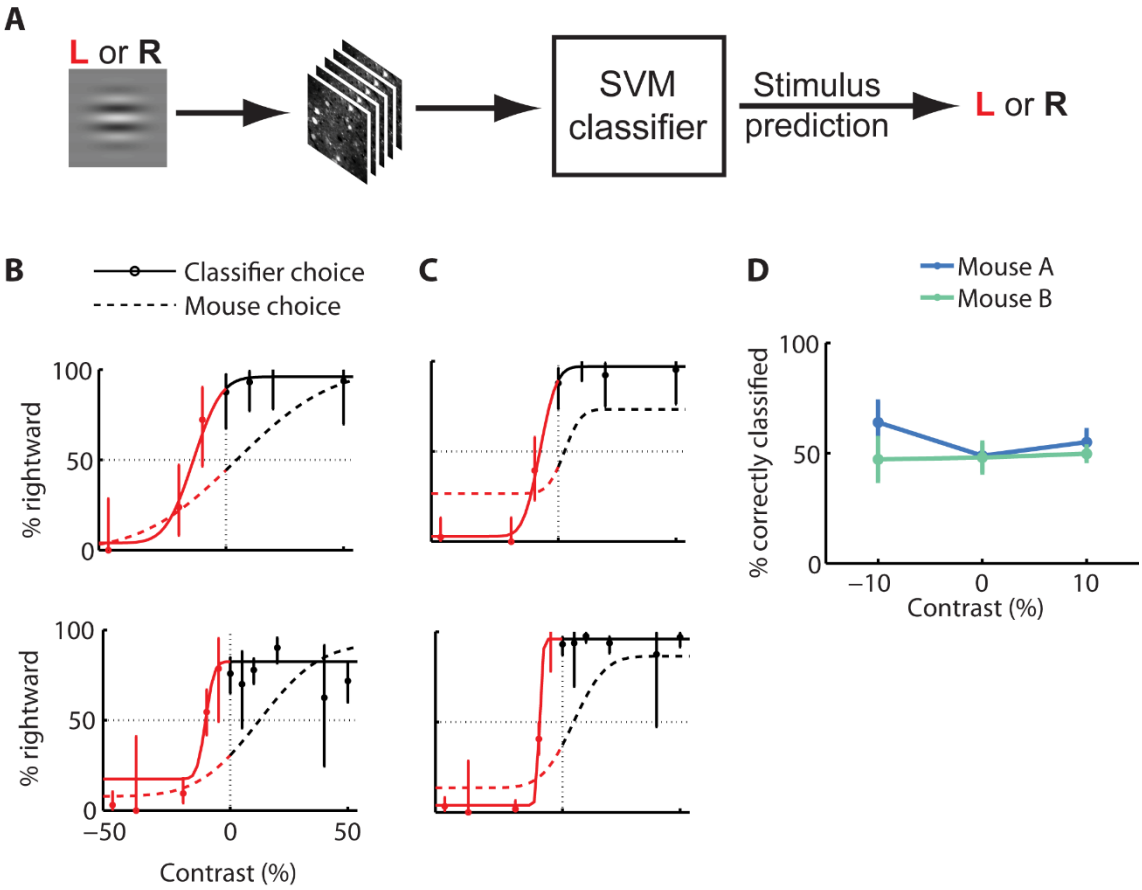

Figure 3-4 Decoding task variables from V1 stimulus responses

A, Schematic of classifier procedure. A support vector machine (SVM) is trained to classify the stimulus position of trials from vectors of calcium imaging movie pixels during the fixed stimulus period (0-1 s following onset). See main text for details. ***B***-***C***, Population neurometric functions for contrast (solid lines) for two mice (row-wise). Trial stimulus position classifications made by SVMs shown as a function of contrast. A classifier was trained on half the trials within a session and tested on the other half (***B***). The same classifier was then tested on sessions from two other days (***C***). Error bars are 95% binomial confidence intervals. For comparison, the psychometric functions obtained from the mouse choices on the same trials are shown (dashed line). ***D***, Classifier performance on decoding mouse choices (cross-validated). SVMs were trained on response movies as in ***A*** but in this case to classify mouse choices on a subsets of trials with the same stimulus condition (stimulus-intendent). Error bars show standard deviation obtained by classifying random subsets of trials.

In order to assess the relationship between sensory coding and mouse choices, I tried to decode choice from stimulus-independent population activity. To do this, I trained and tested SVM choice classifiers among trials with the same stimulus contrast and position. As with the position classifiers, I first trained and tested choice SVMs on vectors of stimulus response frames. However, choice classification performance was not significantly different from chance level (Figure 3-4C). I also explored decoding choice from neural activity processed in different ways. I tested SVMs trained on just the final calcium frames of the stimulus response (the frame just before the stimulus became interactive), or directly on traces from cells. I also tested SVMs trained on neural activity leading up to (and aligned with) the onset of turns. However, none of these variations yielded above chance-level performance. The failure to decode mouse choices suggests that the choice variability for a given stimulus condition was not significantly related to variability in the V1 activity that we recorded.

Task-related pre-stimulus calcium activity

Having observed that calcium activity was typically elevated at stimulus onset time and subsequently decayed if ipsilateral or blank stimuli were presented (Figure 3-3B), I wanted to characterise this pre-stimulus activity and understand how it was related to behaviour.

During this period there was a build-up in calcium activity, which was clear in trial averages (Figure 3-5) but also apparent as individual events (indicated by asterisks in Figure 3-2C). The increase was smaller in amplitude than subsequent

stimulus responses but reliable across cells (pre-stimulus increases were 4.3±3.1% vs 18%±16% stimulus Δ*F*/*F*).

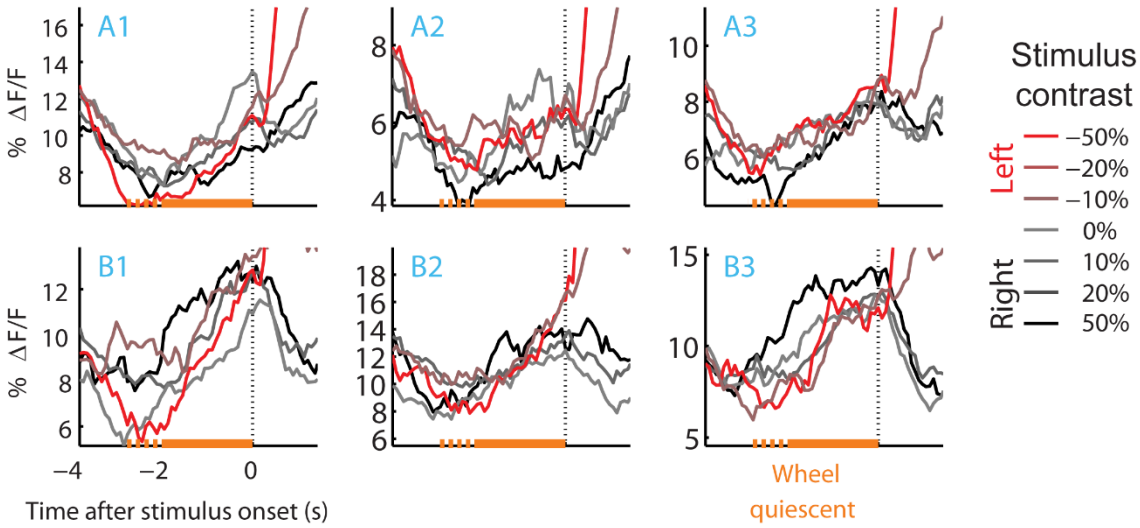

Figure 3-5 V1 activity grows in anticipation of the stimulus

Focus on pre-stimulus calcium activity from the same cells (blue codes of each panel) and sessions as in Figure 3-3. Orange bar indicates 2-3 s no wheel movement (*quiescent*) period (solid portions indicate no movement in all trials; dashed portions indicate movement on some trials). Plot line colours indicate the contrast and position of stimulus presented at time zero (see legend).

Mice were relatively still during the pre-stimulus period as stimuli were only presented after mice had not turned the wheel throughout a 2-3 s window (quiescent period). Presumably reflecting this task structure, mice generally made wheel turns in extended bouts with extended intervening periods of non-movement (Figure 3-2D) throughout a session. From inspecting calcium and wheel velocity traces, it appeared that the pre-stimulus calcium increases occurred specifically during non-movement periods and were truncated with the onset of turn bouts (for example, compare the events indicated by crosses in Figure 3-2C with the wheel velocity trace in Figure 3-2D).

To better characterise the movement bouts and their relationship with pre-stimulus activity, I analysed calcium activity around the onsets and offsets of the bouts. I first fitted movement bout intervals using a dynamic thresholding procedure (Schmitt trigger) on the wheel speed traces. From these I obtained times of their onsets and offsets (green and red arrows, respectively, in Figure 3-2D). The distribution of non-movements periods reflected the timing of the 2-3 quiescent period with a mode at ~3 s (lower panel in Figure 3-6A). However, in many cases mice made premature movements giving intervals that fell short of the quiescent period on particular trials and delaying stimulus presentation. I calculated bout onset- and offset-triggered averages from non-stimulus periods of cell calcium traces (for method details, see Data analysis). I found that nearly all cells showed similar average courses around bout onset and offset times: the activity of most cells peaked at the onset of bouts then decayed (Figure 3-6B) but started from a trough at the offset of bouts and increased (Figure 3-6C). Averages across all cells for onsets and offsets reveal the same trend across two mice (Figure 3-6D).

To assess whether this pre-stimulus activity was related to movement in a similar way to V1 modulation by locomotion (Saleem et al., 2013), I performed the same analysis on naïve mice imaged while running in the dark. This time I fitted onsets and offsets to bouts of running, and calculated triggered calcium averages on those events. In contrast to task movement-related activity, the activity of most cells increased from a trough at onset of running (Figure 3-6E) and decreased from a peak with at offset of running (Figure 3-6F), and the averages across cells reflected this pattern (Figure 3-6G).

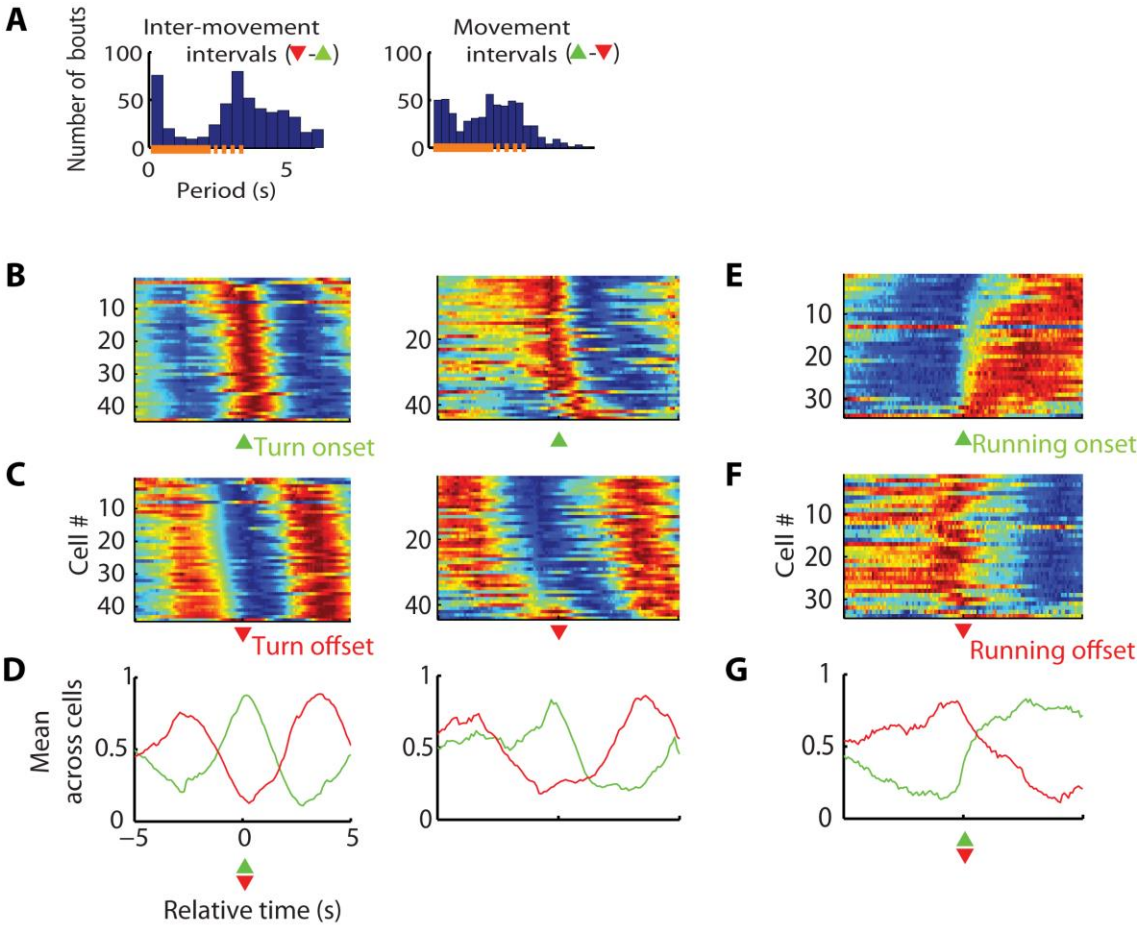

Figure 3-6 Pre-stimulus V1 activity during correlated with wheel turns

A, Distributions of movement bout durations (upper panel) and inter-movement intervals (lower panel) ***B***, Non-stimulus calcium activity triggered on wheel turn onsets (upper panel) and turn offsets (lower panel) for 45 cells (plot rows) in two mice (left and right panels). Each row is normalised to range from its minimum and maximum, and are sorted by turn offset amplitude at -1 s. ***C***, Mean turn-triggered averages across cells in each mouse. ***D***, ***E***, Similar analysis for a naïve mouse running in the dark.

In each recording session, we took averages over the field of view to obtain a global measure of activity, then used the amplitude of this activity just prior to stimulus onset, the pre-stimulus *baseline*, to divide trials into high and low baseline trials (Figure 3-7A). Stimulus responses as a function contrast were generally larger

for high baseline trials compared to low baseline trials suggesting that stimulus responses were additive with the baseline responses (Figure 3-7B).

Given that pre-stimulus activity affected sensory responses, I next asked whether there was any relationship between the pre-stimulus activity and task performance. I computed separate psychometric functions for high and low baseline trials (Figure 3-7D) and found that across most sessions, contrast thresholds were lower for high baseline trials (Figure 3-7E). Furthermore, we found that overall accuracy of choices was better in high than low baseline trials in 8/9 sessions (Figure 3-7C).

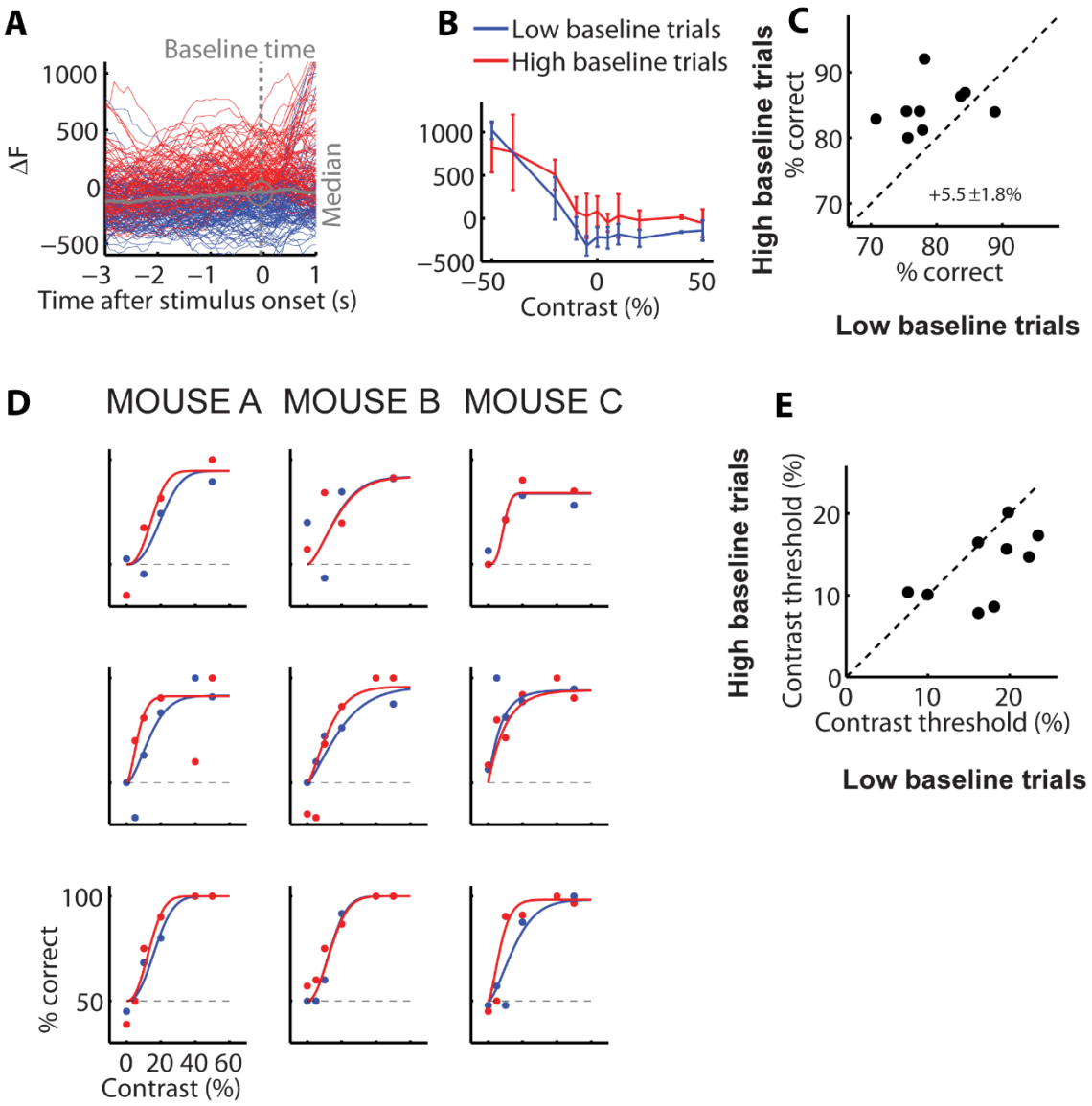

Figure 3-7 Pre-stimulus baseline activity in V1 predicts task performance

A, Calcium activity pre- and post-stimulus onset over the field of view from a single session. Traces show Δ*F* of individual trials, colour-coded according to whether they were categorised as high or low baseline trials (see legend). The trials were categorised by thresholding their amplitude at baseline (the moment at the grey dashed line) with the median baseline amplitude (grey circle), creating two equally sized sets. ***B***, Contrast response amplitudes from the same data as in ***A*** grouped by baseline category. ***C***, Comparison of choice accuracy on high versus low baseline trials on nine recording sessions (three mice on three days each). ***D,*** Contrast psychometric functions from trials grouped by baseline amplitude for three recording sessions (row-wise) of three mice (column-wise). Percent correct is plotted as a function of *unsigned* contrast (i.e. stimulus position is not differentiated). ***E***, Comparison of task contrast thresholds from psychometric fits in ***D***.

3.4 Discussion

I imaged populations of cells in V1 of mice performing a psychophysical task. During a typical imaging session, mice performed hundreds of trials and from these, I was able to obtain high-quality psychometric functions of contrast. This allowed me to compare neural responses with behavioural reports to the same stimuli and to assess non-sensory contributions to V1 activity and relate them to task variables.

Calcium transients signalled via GCaMP6m were typically large in amplitude and had mostly decayed between trials, consistent with the known timing of GCaMP6 activity (Chen et al., 2013). I could identify cells with strong calcium responses to contralateral task stimuli that were modulated by contrast, consistent with typical responses to gratings in mouse V1 (Van den Bergh et al., 2010).

Using a support vector machine (SVM) classifier, I was able to obtain estimates of population neurometric functions for contrast and compare them to psychometric functions obtained on the same subsets of trials. The neurometric functions typically had lower contrast thresholds than the corresponding psychophysical thresholds and classification accuracy was robust across sessions, consistent with previous studies comparing neuronal and psychophysical performance when extrapolated to multiple neurons (Britten et al., 1992; Busse et al., 2011; Mountcastle et al., 1990; Stüttgen and Schwarz, 2008; Tolhurst et al., 1983; Vogels and Orban, 1990)

In contrast to position decoding, I was unable to decode mouse choices from stimulus-independent differences in V1 calcium activity. In general, if noise in sensory neurons plays a causal role in subsequent decision-making processes then stimulus-

independent variability in their activity should be correlated with choices. If this was the case in these experiments, then it should be possible to decode choices from stimulus-independent activity in V1. However, there are a number of possibilities for why the SVM decoding approaches that I tried failed.

Because I trained and tested classifiers among trials with the same stimulus, the number of trials available was relatively low when compared to the dimensionality of the data used for training (which were vectors of pixels from imaging frames). This suggests that successful decoding of choice might have been achieved if data from five times (or more) as many trials were available combined with dimensionality reduction of the training data. A good starting point for the latter would be to use principal component analysis. This may be effective with cellular calcium data given the spatial and temporal redundancy introduced by relatively slow calcium transients from sources which are typically spatially extended, as compared with photon shot noise for example, a major noise source in two-photon imaging, which is independent in space and time.

I only tested decoding choice with linear SVMs in order to retain a straightforward interpretation of any classification models obtained (Haasdonk, 2005). However, it is possible that non-linear kernel SVMs, or indeed other learning algorithms might perform better at classifying choice. Better decoding results might be obtained by attempting to predict choice using a single model across trials of all stimulus conditions. Such an approach would still need to separate the neural variability explained by the stimulus from that explained by choice alone.

Another factor for decoding choice is the distribution of any sensory neurons that inform subsequent decision-making. Two important questions are whether it is expected to find choice probabilities in V1, and whether the task is V1 dependent. Most studies looking at this have been performed in primates, and compared to what has been observed in higher visual areas, many have found choice probabilities to be either modest or absent in V1 (Grunewald et al., 2002; Leopold and Logothetis, 1996; Nienborg and Cumming, 2006). However, in these studies, task discriminations involved either depth or motion, quite different to the task used here. In tasks involving orientation discrimination, significant choice probabilities were observed in V1 (Nienborg and Cumming, 2014). Furthermore, weak but significant choice probabilities were observed in a Gabor grating detection task arguably comparable to the task used here (Palmer et al., 2007). Addressing the second question, on V1 dependence of this task, in Chapter 4 (V1 inactivation during the task), I show preliminary data from inactivation experiments that indicates that V1 is required for performing the task, which implicates activity of V1 neurons in subsequent decision processes.

If decisions were informed by a much larger pool of V1 neurons than were imaged, the amount of choice-related information in the imaged population would be small and hard to detect. At the other extreme, if very few V1 neurons were causally involved in decision-processes, it would be unlikely that I was imaging the relevant neurons. In both cases, recording simultaneously from more neurons and over different cortical depths would help overcome these factors. This is already possible to some degree with improved two-photon microscopes.

An alternative origin for choice-related activity in sensory neurons is top down influences from brain state and decision processes, as opposed to sensory noise that plays a causal role in the decisions themselves (Nienborg and Cumming, 2009). In this case, the time course of any choice-related activity will be more related to internal events and behaviour than sensory events. While I also failed to decode choices from calcium activity aligned to the onsets of choices (specifically to turn onsets), this was specifically from activity preceding the turns. It is possible that this activity window is too early to see top-down modulation related to choice. This window was chosen in order to control for stimulus movement that usually accompanied the turns. A later window could be used if analysis was restricted analysis to those trials where choices started while the stimulus was still fixed. However, this is undesirable as it would further reduce the number of usable trials. Alternatively, using faster indicators such as GCaMP6f (Chen et al., 2013) or recording electrical activity could help to see any top-down modulation that is present in V1 earlier in the recording. Finally, modifying the task design could allow later windows to be used. I have already had some preliminary success with abolishing stimulus interactivity once mice are proficient.

It is also possible that the choices of the mice were not dependent on information from V1. The information used for decision-making may bypass V1 in this task, particularly in highly trained animals like we recorded from. For example, it may originate from pathways parallel to V1 (Morin and Studholme, 2014), such as in superior colliculus. However, preliminary results from optogenetic inactivation suggest that choices in this task do indeed depend on contralateral V1 (see *V1 inactivation during the task* in Chapter 4).

Some of these factors could lead to stimulus-independent variability being small in early visual areas such as V1. However, this would implicate would other brain areas (those involved in later stages of decision-making) in introducing the behavioural variability that we could not account for by variability in V1. It would be straightforward to apply the same techniques described here to look for stimulus-independent choice-related activity in other brain areas. A promising candidate is posterior parietal cortex (PPC). It is known to be involved in rodent decision-making (Erlich et al.; Hanks et al., 2015; Harvey et al., 2012). In primate studies, PPC has been shown to play a role in visually guided goal-directed behaviours (Glimcher, 2003; Gnadt and Andersen, 1988; Scherberger and Andersen, 2007). Finally, mouse PPC may overlap with one or more higher visual areas tuned for moving stimuli (Andermann et al., 2011; Marshel et al., 2011). Taken together these results suggest PPC might be particularly relevant for this task.

Finally, we also discovered non-stimulus activity in V1 and could relate it to task performance. We observed relatively small but significant increases in calcium activity during the pre-stimulus period. In the task, a wheel quiescent period required before stimulus presentation was deliberately introduced in order to control for wheel movements at stimulus onset. However, in relation to this activity, introducing this period had the unintended effect of making quiescent periods and stimulus anticipation indistinguishable. Since wheel quiescence was predictive of forthcoming stimuli, even quiescent periods which were too short to initiate trials could legitimately be accompanied by stimulus anticipation until the abortive movements are actually made. Nonetheless, we found that the amplitude of this activity

(averaged over the field of view) just prior to stimulus onset (the pre-stimulus baseline) was predictive of subsequent psychophysical performance: high baseline trials were accompanied with lower contrast thresholds and more accurate choices. Further investigation is needed to understand the basis of this pre-stimulus activity, and this is currently the subject of investigation. Single-unit electrical recordings are planned to investigate whether the calcium increase is also associated with increased spiking. Separate experiments are planned with GCaMP targeted to specific neuron types (excitatory or inhibitory neurons, or even more specific subclasses) to investigate whether the activity is present only within specific cell types.

A major benefit of using GCaMP is the ease of longitudinal imaging. I took advantage of this to image more trials with the same field of view over multiple sessions. This could be further exploited to obtain many more trials to improve statistical power for trial-based analyses (for example as proposed above to improve choice decoding performance). In practice however, I was faced with time limits on recording as cell health and recording quality deteriorated over the course of increasing GCaMP expression (noticeable 4-6 weeks post injection). Reports and preliminary findings suggest this may be improved by careful titration of injected virus concentration. Alternatively, using transgenic mouse lines for GCaMP offers pharmaceutical control over the induction time of GCaMP expression and may provide more stable expression over longer periods (Madisen et al., 2015). Being able to carry out longitudinal imaging also enables probing the effects of task learning on stimulus and non-stimulus related neural activity. While we did not study this

question, the behavioural and recording techniques I have presented are well suited to addressing it.

In summary, I have shown that using the task I developed with a well suited neural recording method combine to a powerful technique for studying the relationship between perception and decision and their underlying neural activity. These results have replicated the methodology and some the results of similar studies performed in primates (Britten et al., 1992, 1996; Newsome et al., 1989b). However, armed with some of the powerful genetic tools available only in the mouse model, including cell class-targeted measurements and manipulations (Luo et al., 2008), more insightful dissections of the neural circuits underlying perception will be possible using these techniques.

4 A versatile framework for perceptual decision-making tasks

As I showed in Chapter 2, performance in the interactive wheel task was largely consistent across the different versions that I tested, despite significant changes to the stimuli used and task timing. Here I briefly present preliminary results from a number of other variants that have been developed to probe different questions.

Contrast discrimination and a no go option

In collaboration with Nick Steinmetz (Steinmetz et al., 2015), we gave mice a contrast discrimination task, in which gratings were simultaneously presented on the left and right of the screen and mice were rewarded for bringing the highest contrast grating to the centre. In addition to left and right choices, mice were also given a no go option: if a left or right response was not completed within 1.5 s after stimulus onset, it was counted as a no go trial. No go responses were the only rewarded responses for zero contrast trials.

These two modifications are both aimed at obtaining more detailed psychometric measurements to understand the strategy used by mice, and ultimately to relate these more precise measures to neural activity. Presenting two stimuli with independently varied contrast enables behavioural sensitivity to stimulus contrast in each position to be estimated. This can for instance highlight a strategy of just paying attention to stimuli in one position. Such a strategy is also discouraged with discrimination: just reporting the presence or not of the stimulus on one side (and

ignoring the other) can be very effective when it only appears on one side at a time, but it will not work when half the time a stronger stimulus (predicting reward) is on the other side. Offering a no go option (and rewarding it for blank trials) can potentially allow a direct measurement of the percept not seeing any stimulus. Relating such percepts to neural activity is not possible in the standard task, and such an analysis might uncover choice correlations.

In this task, mouse choices were attentive to the contrast of both stimuli: they typically reported the position with the highest contrast (Figure 4-1A). Furthermore, they also learned to withhold responses on blank trials. They also (incorrectly) withheld responses on other trials, but this was more common on the lowest contrast trials.

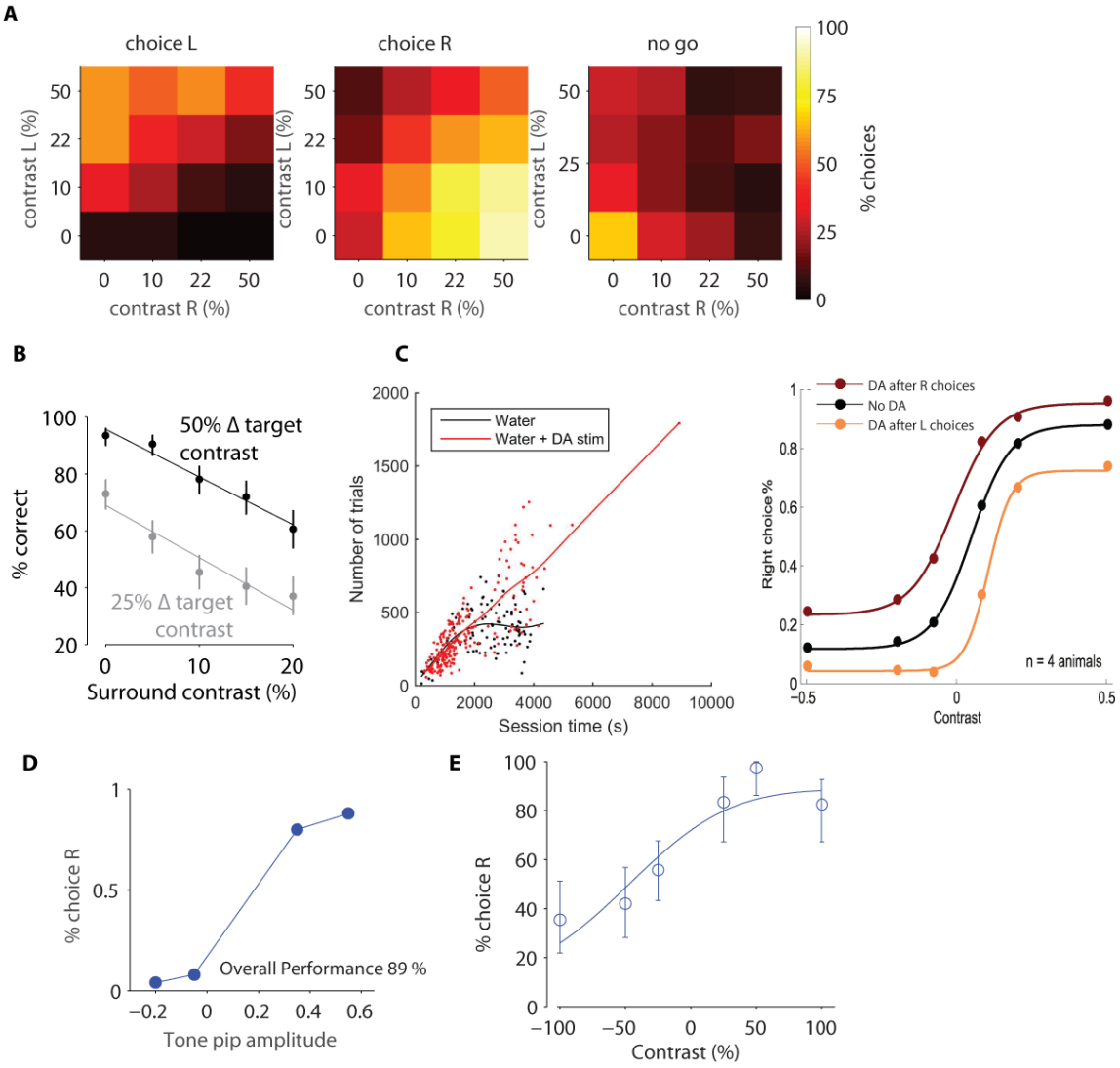

Figure 4-1 Interactive wheel task variants

See main text for more details. ***A***, Contrast discrimination between left and right gratings adding a no go choice option. Proportions of three choice made shown as functions of left and right contrast. ***B***, Contrast discrimination with surround suppression and *no go* choice. Percent correct for two target grating contrast differences as a function of surround contrast. Note here chance level is ~33%. ***C***, Grating detection with optogenetic stimulation of midbrain dopamine (DA) neurons. Left panel, Number of trials completed versus session time for sessions with and without DA stimulation. Right panel, Contrast psychometric functions comparing choices on trials following DA stimulation of left or right choice trials, or trials with DA stimulation. ***D***, Tone frequency discrimination task. Percentage of right turns made as a function of signed auditory amplitude (low frequency onsets are positive). Mice are presented a stream of tone pips (5 pips/s) onset at a low or high frequency. Mice could increase the tone frequency by turning the wheel right, or decrease it by turning it left. A target "home" frequency was rewarded ***E***, Gabor rotation

task. Percentage of right turns made as a function of signed contrast (45° onset orientations are positive). Mice were presented with a grating at +45° o -45°, which they can rotate left or right with the wheel. They were rewarded for making it horizontal but were timed out for making it vertical.

Surround suppression

In collaboration with Miles Wells, we modified the task to assess the psychophysical effects of surround suppression. Surround suppression is a phenomenon whereby the stimulation of visual cortical neuron's receptive field surround can attenuate its response to a stimulus in the centre of its receptive field (Born and Tootell, 1991; Jones et al., 2001). Surround suppression has been shown in mouse visual cortex, where it is sensitive to behavioural factors, such as locomotion (Ayaz et al., 2013)

In this study, we wanted to assess how contrast discrimination performance is modulated by surround stimulation, with the ultimate goal to relate this directly to suppression of neuronal responses (planned for future experiments). As with the previous task, bilateral gratings were presented with independent contrasts, and reward was given for selecting the highest contrast grating. A no go option was available and rewarded for zero contrast. In addition, a full field surround was present in the background. For a given target contrast difference, performance decreased linearly as a function of surround contrast with similar gradients but with a downward shift for the smaller contrast difference (Figure 4-1B).

Midbrain dopamine stimulation

In collaboration with Armin Lak (Lak et al., 2015), optogenetically stimulated dopaminergic (DA) neurons in ventral tegmental area of mice while they performed

the task. We wanted to investigate whether the addition of DA stimulation would increase motivation levels for mice, and whether it could be used to bias choices.

Mice tended to stay motivated on longer sessions with more trials when they received DA stimulation in addition to water reward (Figure 4-1C, left panel). Compared to water reward-only trials, when mice received DA stimulation following correct left choices, choices on subsequent trials were biased to the left, and when they received DA stimulation following correct right choices, subsequent choices were biased to right (Figure 4-1C, right panel).

These results suggest that DA stimulation can provide a strong additional motivation to increase the number of trials mice will do on this task, similar to that seen with electrical stimulation of dopamine-releasing neurons in rodents (Olds and Milner, 1954). We are currently investigating whether DA stimulation alone, without the need for water reward (and therefore without the need for water restriction), can provide the required motivation for mice to perform this task.

Tone frequency discrimination task

In collaboration with Elina Jacobs, we trained mice in a task using auditory stimuli instead of visual. We wanted to develop an auditory analogue of the visual interactivity in the standard task, and wanted to use stimuli that would have an analogous representation in auditory cortex. We assumed that this might help mice to learn a 2AFC auditory task, to make results more comparable with those from the visual task, and be ultimately suited to investigating multisensory processing in combination with the visual task. Since mouse auditory cortex is organised

tonotopically (Bandyopadhyay et al., 2010), analogous to retinotopy in visual cortex, we decided to use task stimuli where mice had to discriminate between sounds of different frequencies, and would have to move within frequency space by turning the wheel.

Mice were presented with a regular train of tone pips (5 pips/s). Mice could change the tone frequency by turning the wheel. The frequency was scaled logarithmically with wheel angle, decreasing it with left turns, increasing it with right turns. Tone pips began with at a high (32 kHz) or low frequency (8 kHz) at onset, and mice were rewarded for tuning the frequency to an intermediate "home" frequency (16 kHz) where the frequency would lock and the pips would continue during the 1-2 s feedback period. Turning the same angle in the wrong direction would also lock the frequency while the mice received a 2 sec timeout with a white noise sound.

Mice learned to perform the task to high accuracy, correctly responding by shifting the tone pip frequency up or down depending on whether it started higher or lower than the target frequency. However, their choices tended to be biased, presumably due to frequency-dependent hearing thresholds. This highlights a potential problem with combining auditory frequency discrimination with modifying task difficulty by changing tone amplitude: hearing thresholds at each frequency need to be matched to such prevent biases. Improvements to this paradigm for obtaining psychometric measurements are currently under development.

V1 inactivation during the task

In collaboration with Nick Steinmetz, we optogenetically inactivated left or right V1 on a subset of trials during a session. Mice were trained on the task with the no go option (see above) but single gratings were only presented on one side or the other on each trial. During training, mice were rewarded for making no go responses on trials with no grating presented. Training mice to report not seeing a stimulus is a powerful method when combined with an inactivation manipulation since it enables distinction to be made between motor and perceptual biases versus eliminating a percept entirely.

To inactivate visual cortex, mice with channelrhodopsin in parvalbumin positive interneurons had focal illumination from a laser to their left or right V1 during stimulus periods on some trials. On left V1 inactivation trials (Figure 4-2, top panel, solid lines), the mouse chose the right hand grating much less often (solid vs dashed orange), usually responding no go instead (solid vs dashed black), but its choices to the left grating were largely unaffected (solid vs dashed blue). In contrast, on right V1 inactivation trials (Figure 4-2, bottom panel), the opposite was true: the mouse chose the left hand grating much less often (solid vs dashed blue), choosing no go instead (solid vs dashed black), but responses to the right grating were largely unaffected (solid vs dashed orange).

These results suggest that the inactivation was selectively eliminating the percept only of stimuli presented on the contralateral side. The fact that their choices for ipsilateral stimuli were largely unaffected by inactivation, but tended to make a

higher proportion of no go responses to contralateral stimuli strongly supports this conclusion, and demonstrates the strength of this choice paradigm in this context. Finally, it provides strong evidence in favour of V1 dependence for this task.

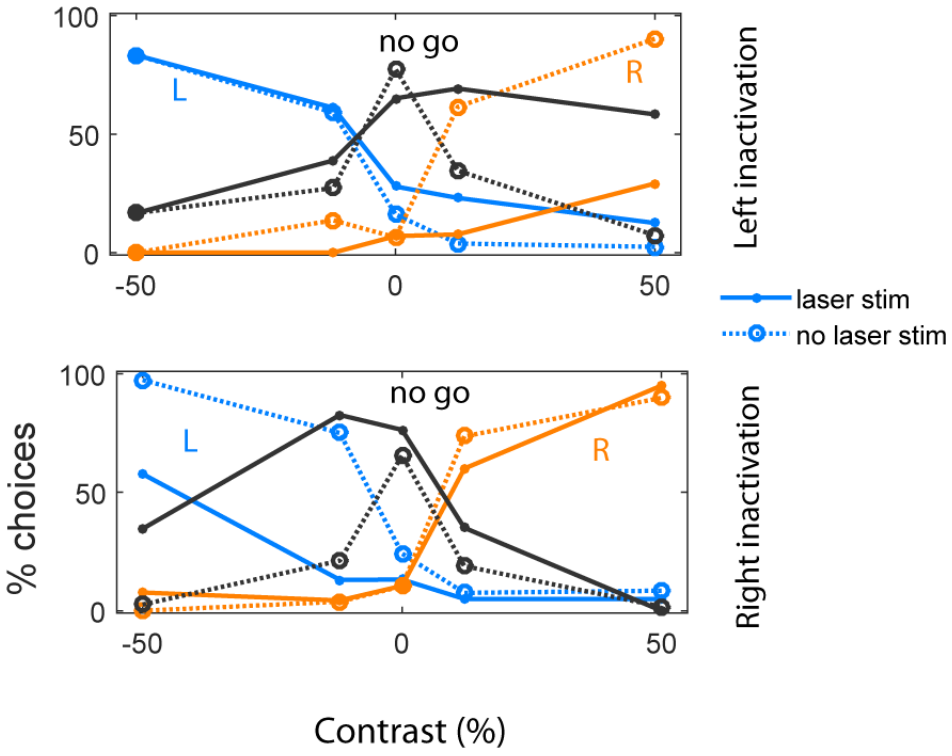

Figure 4-2 Preliminary results from V1 inactivation.

Psychophysical effect of V1 inactivations in mice expressing ChR in parvalbumin interneurons. Percent of each of three different possible choices (blue, left; orange, right; black, no go) shown as a function of signed stimulus contrast (right stimulus contrast minus left stimulus contrast). Choices are further subdivided into whether they made with (solid lines) or without (dashed lines) laser inactivation. Results from inactivation of the left V1 (top panel) and right V1 (bottom) by directing a laser onto V1 during the stimulus period on a subset of trials

DiscWorld: a rotation task for orientation

I developed a rotation analogue of the visual position task for probing orientation psychophysics in mice. In this task, I presented mice with a grating disc

centred on the screen. It was initially presented at -45° or +45° and mice could rotate it by turning the wheel. If the grating was turned toward horizontal its orientation would lock and stay visible for 1 s, while the mouse received a reward. If the grating was turned toward vertical its orientation would lock there and stay visible for 2 s while the mouse was played a white noise sound. Mice were able to perform this task well above chance and their responses as function of contrast were well fit by psychometric curves though often revealing biases (Figure 4-1E). Task acquisition took longer and accuracy on the easiest trials was not as high as for the position task.

From the point of view of measuring V1 responses, the task has a number of potential advantages. First, because there is only one stimulus position, a retinotopically matched region of V1 will respond to every stimulus presented (assuming contrast is high enough). Analyses comparing neuronal activity with animal choices will not be missing potential information from the other cortex. Second, mouse V1 responses are tuned to orientation (Niell and Stryker, 2008) and neighbouring neurons are tuned to different orientations but with similar receptive fields. Thus, neural recordings in a retinotopically matched region of V1 are likely to yield neurons tuned over the range of orientations presented as mice rotate the stimuli. These could be pivotal features for observing neural correlates of perception in V1 that can be characterised, thereby making advances on the motivating questions of this thesis. Further experiments using this task is the subject of ongoing investigation.

4.1 Discussion

I have shown that the basic framework of these tasks enables head-fixed mice to perform two-alternative choice tasks under a variety of specifications. In all the task variants in this thesis, the visual feedback is primarily a teaching aid, and not directly relevant to the scientific question being probed. However, stimulus interactivity could be used specifically to ask questions about the neural basis of orienting behaviour and sensorimotor coding. The relative simplicity of the stimuli and the task design would make it simpler to ask such questions relating to stimuli and movement than in comparable virtual navigation arrangements (e.g. Harvey et al., 2012).

5 General conclusions and outlook

I set out to develop a psychophysical task that mice could perform head-fixed with the aim of measuring neural activity that could be related to their perceptual decisions. After some initial failed approaches, I was able to develop an effective task, and in this thesis I have described it more generally as a versatile framework for teaching mice to perform perceptually guided tasks while head-fixed. The key innovations were using a wheel that mice could turn with their forepaws and enabling them to use it to manipulate the stimulus attributes of interest. I showed the results of the development of this approach at various stages.

A head-fixed two-alternative forced choice task

My starting point was wanting mice to report whether visual stimuli were presented on the left or the right with corresponding wheel turns. First, when I presented stimuli that were only associated with their actions via rewards, mice failed to learn to make turns directed by the stimuli. However, I found that by coupling their wheel turns to stimulus position and rewarding them for centring the stimulus, mice could learn the task to high proficiency. At this stage psychometric analyses of data obtained on this task were robust and informative about psychophysical contrast thresholds and reaction times of mice. However, motivated by considerations of interpreting simultaneously measured neural activity. I further refined the task. Crucial among these were simplifying the stimuli used and adding a period where the stimulus was fixed. In spite of these and other changes, mice were still able to learn. In fact in these later versions, mice learned considerably faster, with above

chance level performance after a week of training, and were producing stable, high quality psychometric data by 2-3 weeks of training. However, this improvement in learning rate could be due to other factors, including more experience with handling mice and a different water restriction schedule. As side note to the main aims, results on the latter demonstrated that the water schedule regime is an important factor in optimising motivation, as the number of days since free water had a large effect on the number of trials completed by mice.

Armed with an effective task, I turned to two-photon GCaMP imaging to record neural activity in V1. This technique offers a number of features suited for behavioural recordings in which significant training is required and recording many trials is desirable. Chief among these is the ability to record activity from populations of neurons over many weeks. Putting all this together, I was able to image V1 calcium activity in mice expressing GCaMP6 over multiple sessions while they performed the position discrimination task. Beyond demonstrating classic sensory responses to task stimuli, analysis of this data provided three key results, and raised some important questions.

Mice performed worse than their V1 neurons

Measurements of population contrast sensitivity exceeded that of the corresponding psychophysical measurements (Burgess et al., 2013). I made these measurements using a support vector machine (SVM) to classify stimulus position (the same task the mouse was performing) from imaging frames. I was able to construct neurometric curves for direct comparison with psychometric curves

obtained on the same trials. This result suggests that not all sensory information was being optimally exploited for decision-making in this task. It raises the question of how sensory information is put to use to inform actions, and what other factors override this. These factors may include non-sensory influences such as recent reward and stimulus history (Busse et al., 2011), committing to actions before processing all available information (Resulaj et al., 2009), and the deleterious effects of neuronal noise (Faisal et al., 2008) and suboptimal inference in downstream decision-making processes (Beck et al., 2012). Finally, further work is needed to investigate what features of the neural activity were important for the classifier's performance, and what this tells us about sensory representations.

Stimulus-independent V1 activity appeared uncorrelated with perceptual decisions

The same SVM-based approach was unsuccessful at decoding mouse choices from stimulus-independent V1 activity (Burgess et al., 2013). Setting aside issues of whether the decoding method itself was ineffective (including whether there was insufficient data for proper classifier training), this result suggests that V1 response variability was unrelated to variability in the mice choices. One explanation that preserves the causal role of V1 sensory responses in informing decisions is that sensory variability is averaged out by downstream processes pooling over sizable populations. Instead, the variability of choices might predominately derive from other areas influencing decisions. This interpretation is supported by the previous result: by pooling relevant information over just a single imaging frame, decoders were able to outperform the mice suggesting a large portion of their choice variability was non-

sensory in origin. An alternative hypothesis is that V1 information is not causally involved in decisions in this task and so V1 response variability cannot influence decisions. For example, information might be derived from non-striate visual pathways. However, this hypothesis conflicts with the preliminary results presented from V1 inactivation during this task, and similar results from V1 inactivation in a contrast detection task (Glickfeld et al., 2013).

Pre-stimulus activity predictive of task performance

There were significant increases in calcium activity that occurred before the onset of stimuli during periods of non-wheel movement (Burgess et al., 2014). The amplitude of this activity at stimulus onset (baseline) was additive with subsequent sensory responses and was predictive of subsequent behavioural performance. On trials with a high baseline, mice tended to exhibit lower contrast thresholds and made more accurate choices. These findings are indicative of an attentional effect , although there has been traditionally been some debate as to the prevalence of attentional modulation in V1, at least in monkeys (Posner and Gilbert, 1999). An important question raised is whether this activity increase is spatially specific, a hallmark of selective attention (Desimone and Duncan, 1995), or represents some more global phasic alertness signal (Raz and Buhle, 2006). It would be straightforward to answer in this paradigm, for example by comparing the amplitudes of stimulus responses to pre-stimulus activity in multiple areas, either by repeating two-photon imaging in different fields of view, or using wide-field imaging.

I have presented a task suitable for investigating the neural correlates perceptual decisions in head-fixed mice. The technique I used to teach mice, giving them control over stimuli of interest, may have wider applicability beyond its use as a learning aid, and could be an interesting topic of investigation in its own right.

I used the task to obtain recordings in V1 simultaneously with perceptual measures. The particular findings I have described have raised a number of questions, but many of the powerful tools available in mouse models offer a way forward for resolving them.

6 Appendices

6.1 Pupil diameter correlated with calcium and task timing

I found that pupil diameter was correlated with various task-related behavioural variables and calcium activity. During a subset of the experiments of presented in 3.3, the mouse's eye was filmed while the mouse performed the task and V1 calcium activity was imaged. Pupil diameter in each frame was computed by fitting an ellipse to the dark area delimited by the pupil. The pupil diameter was approximated by the diameter of the ellipse along its major axis.

Pupil diameter tended to be inversely related to calcium activity (black and green traces, respectively in Figure 6-1A). In particular, the pupil tended to be dilating as calcium activity begins to increase. This can be seen in their cross-correlation, which contains a large negative peak, with the calcium slightly delayed compared to the pupil (Figure 6-1B).

Pupil constriction and dilation also strongly followed the timing of stimulus onsets. The pupil tended to be constricting during the period before stimulus onset (while the wheel was not being moved, see Figure 6-1E for comparison), and dilating from a trough at stimulus onset (Figure 6-1C).

Pupil diameter dynamics were also correlated with wheel turns. The pupil tended to dilate after large wheel turns (compare black pupil trace with blue wheel speed trace in Figure 6-1A). The cross-correlation between pupil diameter and wheel

speed revealed a large positive peak, with pupil lagging behind the wheel (Figure 6-1D).

Because these factors are all correlated together, and there are strong autocorrelations in the timing of task events, it is difficult to pick apart relationships and understand factors which might be driving others. More work will be needed to this, and a particular issue is that the pre-stimulus period is always period with no wheel movement, which causes stimulus onset and wheel movement to be tightly correlated.

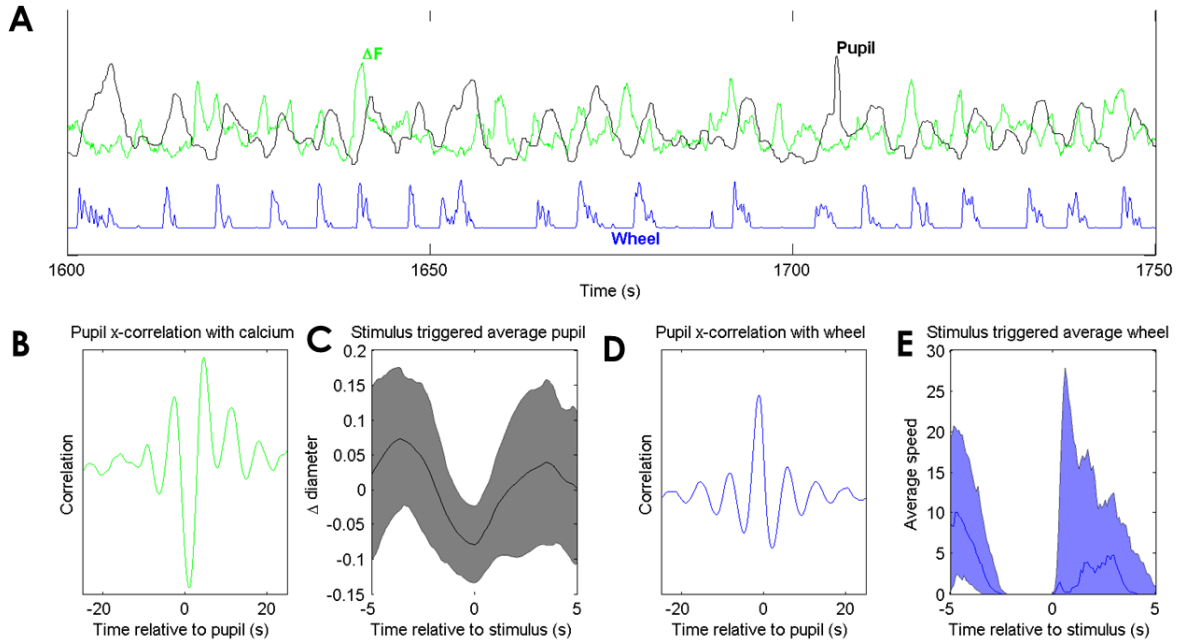

Figure 6-1 Pupil constricts with quiescence

Relationship between calcium activity, pupil diameter and wheel turns during a typical behavioural session. Calcium activity (ΔF) is mean over field of view, with baseline subtracted (baseline computed as described in 3.2).

A, Example traces of ΔF (green line), pupil diameter (black line) and wheel turn speed (blue line). ***B***, Cross-correlation of pupil diameter with ΔF. ***C***, Stimulus onset-triggered average pupil diameter. ***D***, Cross-correlation of pupil diameter with wheel turn velocity. ***E***, Stimulus-onset triggered average wheel turn speed.

6.2 LFP during task performance

Preliminary results from electrophysiological experiments revealed decreased low frequency power during periods of no wheel movement before the mouse responded.

This data is obtained from one mouse in which Michael Okun implanted a 16 channel linear probe chronically into left V1 (Okun et al., 2015). I trained the mouse in version 4 of the grating detection task (see 2.5) and when it reached proficiency, recorded electrical activity while the mouse performed the task. The location of the stimulus at onset was matched to the average retinotopic preference of LFP recorded on the electrode found in separate mapping experiments.

The power of low-frequency oscillations observed in the LFP was highest during wheel non-movement periods, particularly just before onset of wheel movement bouts (Figure 6-2A). An average of the LFP spectrogram triggered on the offsets of wheel turns shows that the power of low frequencies, particularly ~4Hz, tends to increase from a low at the time that the turn stops (Figure 6-2A-D). The time course of this increase follows a similar profile to the build-up in calcium activity in the pre-stimulus period during wheel non-movement (see Figure 3-5 and Figure 3-6). Whether this period is also associated with a change in spike rate, and it's relationship with the calcium build-up is the currently the subject of investigation in planned experiment.

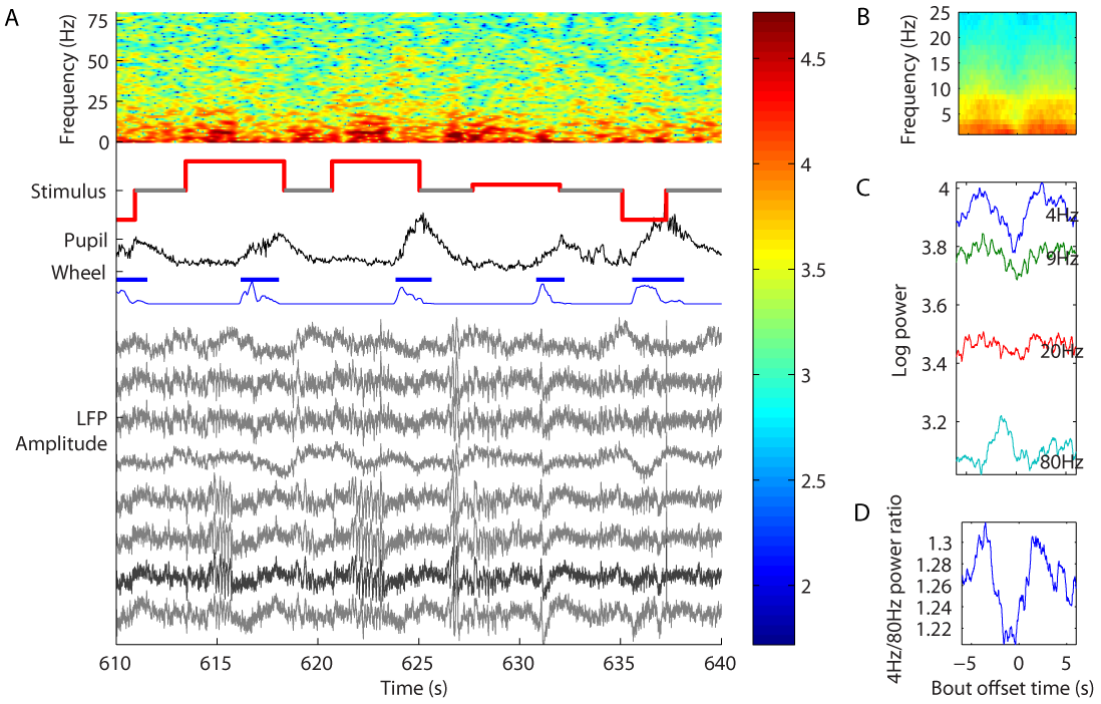

Figure 6-2 Low frequency LFP during wheel quiescence periods

LFP recording while a mouse performed version 4 of the grating detection task.

A, LFP power and amplitude plotted with behavioural events during a typical period in the task. LFP spectrogram (top) is computed from bold LFP trace (bottom). The stimulus trace indicates presence of stimulus on screen when red, where the offset from zero indicates contrast, and sign indicates position (positive is on the right, negative is on the left). Pupil diameter and wheel speed also shown (bars over wheel speed indicate movement bouts). ***B***, Movement bout offset-triggered average LFP spectrogram. ***C***, Power of specific frequency bands from average spectrogram in ***B***. ***D***, Low/high frequency power ratio computed from blue and cyan traces in ***C***.

6.3 Deterioration of GCaMP expression

I found that expression of virally expressed GCaMP tended to be optimal at around 2-3 weeks after injection of the virus, but with expression continuing to increase, over-expression began to be a problem at around 5-6 weeks (Figure 6-3) Optimal expression is characterised by fluorescing soma with dark nucleuses, appearing like "donuts" dominating a field of view (top left, Figure 6-3). Over-expression is characterised by having many fluorescing nucleuses, or "filled" cells (top right, Figure 6-3). Over-expression issues were avoided in the experiments described in chapter 2 by commencing training soon after virus injections. This meant expression was optimal at around 2-3 weeks, by which time the mice were close to proficiency. According to many reports, expression stability may be greatly extended by diluting the virus from stock concentrations.

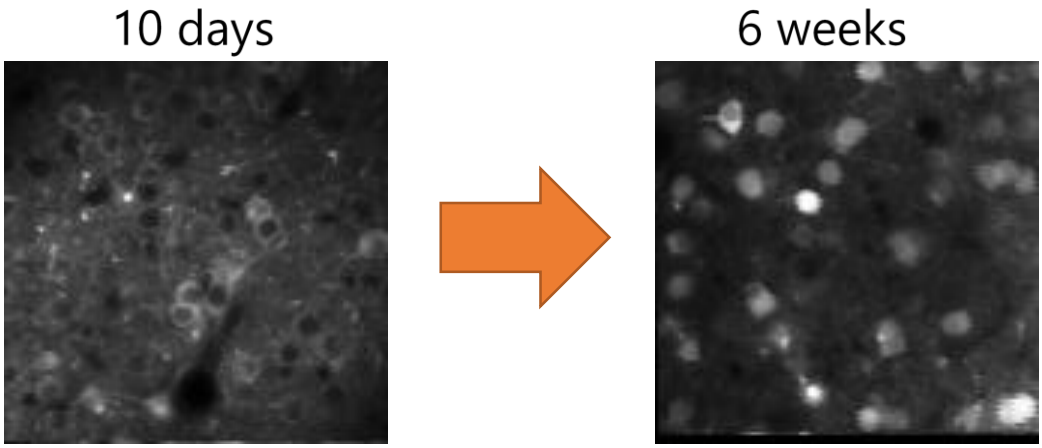

Other examples after 6 weeks:

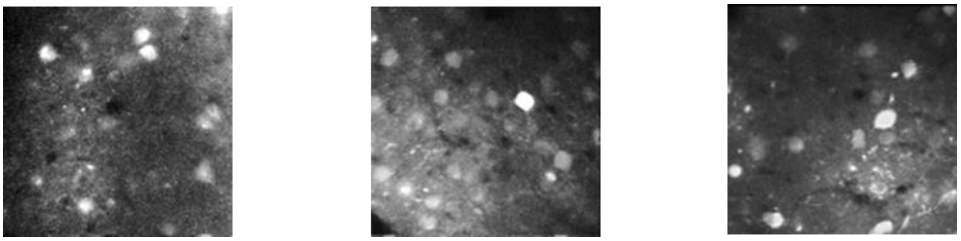

Figure 6-3 Deterioration of GCaMP expression over time

Top, Change in expression quality from 10 days after AAV GCaMP injection to 6 weeks. Bottom, Examples of deteriorated GCaMP expression after 6 weeks from 3 other mice.

6.4 Neurometric classifier bias

Figure 6-4 illustrates how lateralised responses (i.e. responses to stimuli for stimuli on one side, and not the other, as observed in 3.3, see Figure 3-3) produce biased neurometric curves. The figure shows results from a very simple two neuron response model (see caption for more details), which produces an SVM-based neurometric curve with a similar profile to that obtained on actual data in Figure 3-4.

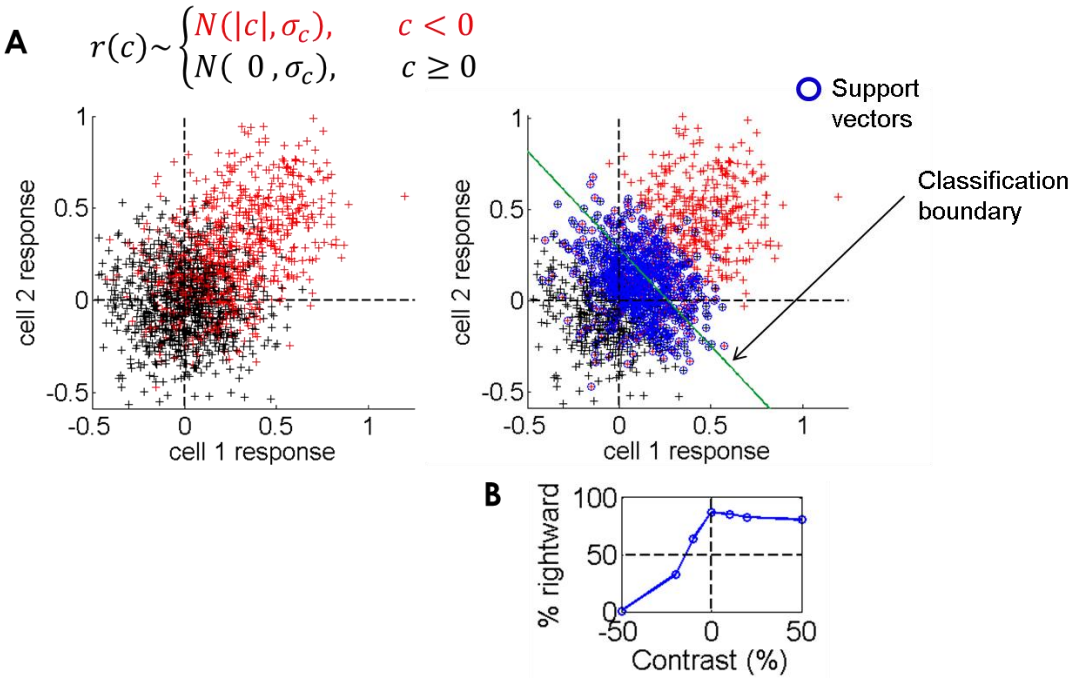

Figure 6-4 Lateralised responses produce classifier bias

Simple neural response model with lateralised modulation by contrast produces biased psychometric curve.

A, Two model neurons produce a noisy response amplitude on each trial that is modulated by the contrast of left stimuli, but unmodulated by right stimuli. Specifically, the response for each trial is drawn from a Normal distribution with a fixed standard deviation, and zero mean for right stimuli (black) and mean of the unsigned stimulus contrast for left stimuli (red; see equation). The left panel shows the response of cell 1 versus cell 2 for each trial, colour coded by the stimulus position. They form two partially overlapping clouds, and the optimal classification boundary obtained by SVM is biased (i.e. it does not pass through the origin, right panel) because the black points (for right stimuli) are zero mean, but the red points have a variable but positive mean. ***B***, The mean classifications of the SVM fitted in ***A*** grouped by trial contrast. As expected, classifications are biased and unmodulated by the contrast of right-hand stimuli, but are modulated by the contrast of left stimuli (since it sets the mean of those responses).

Support

This work was supported by the Wellcome Trust and by the European Research Council. I was supported by a Medical Research Council studentship. Matteo Carandini holds the GlaxoSmithKline/Fight for Sight Chair in Visual Neuroscience. We thank Charu Reddy and Miles Wells for outstanding technical support.

7 Acknowledgments

Firstly, I would like to thank my supervisor, Matteo Carandini. I surely benefited from his tireless support, his cool-headedness and his heroic ability to manage a large lab and still find time for regular (or impromptu) meetings. His eye for aesthetic and in particular his passion to communicate with simplicity and clarity will forever remain an inspiration and a reminder for me to strive to do the same.

I must thank Adam Ranson for his patience and willingness to teach and inspire me in a multitude of techniques and skills. Without his guidance throughout my PhD, I might never have made it.

Aman Saleem, Bilal Haider and Nick Steinmetz will remain an inspiration for their scholarliness and intellectual rigour. Thanks is due to them for great advice, inspiring discussions and their thoughtful approaches. Special thanks must go to Aman Saleem for his interest in my work and for agreeing to hastily proof read my thesis.

It has also been a pleasure to work on projects with Michael Okun, Elina Jacobs and Luigi Federico Rossi. Rossi in particular brought much cheer and air puffs to otherwise laborious experiments.

A big thank you is due Michael Krumin for technical support, but most of all for his tireless sarcasm.

I would also like give a special thank you to Charu Reddy and Miles Wells for their tireless work in keeping the lab running smoothly, yet still bringing liveliness and merriment to the lab.

Finally, thank you to Gemma Callander, for putting up with me during my PhD.

8 References

Andermann, M.L., Kerlin, A.M., and Reid, R.C. (2010). Chronic cellular imaging of mouse visual cortex during operant behavior and passive viewing. Front. Cell. Neurosci. *4*, 3.

Andermann, M.L., Kerlin, A.M., Roumis, D.K., Glickfeld, L.L., and Reid, R.C. (2011). Functional specialization of mouse higher visual cortical areas. Neuron *72*, 1025–1039.

Ayaz, A., Saleem, A.B., Schölvinck, M.L., and Carandini, M. (2013). Locomotion Controls Spatial Integration in Mouse Visual Cortex. Curr. Biol. *23*, 890–894.

Bandyopadhyay, S., Shamma, S.A., and Kanold, P.O. (2010). Dichotomy of functional organization in the mouse auditory cortex. Nat. Neurosci. *13*, 361–368.

Barlow, H.B., and Levick, W.R. (1969). Changes in the maintained discharge with adaptation level in the cat retina. J. Physiol. *202*, 699–718.

Beck, J.M., Ma, W.J., Pitkow, X., Latham, P.E., and Pouget, A. (2012). Not Noisy, Just Wrong: The Role of Suboptimal Inference in Behavioral Variability. Neuron *74*, 30–39.

Bock, D.D., Lee, W.-C.A., Kerlin, A.M., Andermann, M.L., Hood, G., Wetzel, A.W., Yurgenson, S., Soucy, E.R., Kim, H.S., and Reid, R.C. (2011). Network anatomy and in vivo physiology of visual cortical neurons. Nature *471*, 177–182.

Boneau, C.A., Holland, M.K., and Baker, W.M. (1965). Color-Discrimination Performance of Pigeons: Effects of Reward. Science *149*, 1113–1114.

Born, R.T., and Tootell, R.B. (1991). Single-unit and 2-deoxyglucose studies of side inhibition in macaque striate cortex. Proc. Natl. Acad. Sci. *88*, 7071–7075.

Brainard, D.H. (1997). The Psychophysics Toolbox. Spat. Vis. *10*, 433–436.

Britten, K.H., Shadlen, M.N., Newsome, W.T., and Movshon, J.A. (1992). The analysis of visual motion: a comparison of neuronal and psychophysical performance. J. Neurosci. Off. J. Soc. Neurosci. *12*, 4745–4765.

Britten, K.H., Newsome, W.T., Shadlen, M.N., Celebrini, S., and Movshon, J.A. (1996). A relationship between behavioral choice and the visual responses of neurons in macaque MT. Vis. Neurosci. *13*, 87–100.

Burgess, C.P., Ranson, A., Harris, K.D., Linden, J.F., and Carandini, M. (2013). Two-photon imaging of population activity in mouse visual cortex during a 2AFC

task. In Neuroscience 2013 Abstracts, (San Diego, CA: Society for Neuroscience), p. 262.08/PP19.

Burgess, C.P., Ranson, A., Linden, J.F., Harris, K.D., and Carandini, M. (2014). Correlates of anticipation and movement in mouse visual cortex. In Neuroscience 2014 Abstracts, (Washington, DC: Society for Neuroscience), p. 818.07/FF6.

Busse, L., Ayaz, A., Dhruv, N.T., Katzner, S., Saleem, A.B., Schölvinck, M.L., Zaharia, A.D., and Carandini, M. (2011). The Detection of Visual Contrast in the Behaving Mouse. J. Neurosci. *31*, 11351–11361.

Carandini, M., and Churchland, A.K. (2013). Probing perceptual decisions in rodents. Nat. Neurosci. *16*, 824–831.

Cardin, J.A., Carlén, M., Meletis, K., Knoblich, U., Zhang, F., Deisseroth, K., Tsai, L.-H., and Moore, C.I. (2009). Driving fast-spiking cells induces gamma rhythm and controls sensory responses. Nature *459*, 663–667.

Chen, T.-W., Wardill, T.J., Sun, Y., Pulver, S.R., Renninger, S.L., Baohan, A., Schreiter, E.R., Kerr, R.A., Orger, M.B., Jayaraman, V., et al. (2013). Ultrasensitive fluorescent proteins for imaging neuronal activity. Nature *499*, 295–300.

Cortes, C., and Vapnik, V. (1995). Support-vector networks. Mach. Learn. *20*, 273–297.

Desimone, R., and Duncan, J. (1995). Neural Mechanisms of Selective Visual Attention. Annu. Rev. Neurosci. *18*, 193–222.

Dombeck, D.A., Harvey, C.D., Tian, L., Looger, L.L., and Tank, D.W. (2010). Functional imaging of hippocampal place cells at cellular resolution during virtual navigation. Nat. Neurosci. *13*, 1433–1440.

Erlich, J.C., Brunton, B.W., Duan, C.A., Hanks, T.D., and Brody, C.D. Distinct effects of prefrontal and parietal cortex inactivations on an accumulation of evidence task in the rat. eLife *4*.

Faisal, A.A., Selen, L.P.J., and Wolpert, D.M. (2008). Noise in the nervous system. Nat. Rev. Neurosci. *9*, 292–303.

Glickfeld, L.L., Histed, M.H., and Maunsell, J.H.R. (2013). Mouse Primary Visual Cortex Is Used to Detect Both Orientation and Contrast Changes. J. Neurosci. *33*, 19416–19422.

Glimcher, P.W. (2003). The Neurobiology of Visual-Saccadic Decision Making. Annu. Rev. Neurosci. *26*, 133–179.

Gnadt, J.W., and Andersen, R.A. (1988). Memory related motor planning activity in posterior parietal cortex of macaque. Exp. Brain Res. *70*, 216–220.

Gold, J.I., and Shadlen, M.N. (2007). The Neural Basis of Decision Making. Annu. Rev. Neurosci. *30*, 535–574.

Grinvald, A., Lieke, E., Frostig, R.D., Gilbert, C.D., and Wiesel, T.N. (1986). Functional architecture of cortex revealed by optical imaging of intrinsic signals. Nature *324*, 361–364.

Grunewald, A., Bradley, D.C., and Andersen, R.A. (2002). Neural Correlates of Structure-from-Motion Perception in Macaque V1 and MT. J. Neurosci. *22*, 6195–6207.

Guizar-Sicairos, M., Thurman, S.T., and Fienup, J.R. (2008). Efficient subpixel image registration algorithms. Opt. Lett. *33*, 156–158.

Haasdonk, B. (2005). Feature space interpretation of SVMs with indefinite kernels. IEEE Trans. Pattern Anal. Mach. Intell. *27*, 482–492.

Hanks, T.D., Kopec, C.D., Brunton, B.W., Duan, C.A., Erlich, J.C., and Brody, C.D. (2015). Distinct relationships of parietal and prefrontal cortices to evidence accumulation. Nature *520*, 220–223.

Harvey, C.D., Coen, P., and Tank, D.W. (2012). Choice-specific sequences in parietal cortex during a virtual-navigation decision task. Nature *484*, 62–68.

Histed, M.H., Carvalho, L.A., and Maunsell, J.H.R. (2012). Psychophysical measurement of contrast sensitivity in the behaving mouse. J. Neurophysiol. *107*, 758–765.

Houweling, A.R., and Brecht, M. (2008). Behavioural report of single neuron stimulation in somatosensory cortex. Nature *451*, 65–68.

Huber, D., Petreanu, L., Ghitani, N., Ranade, S., Hromádka, T., Mainen, Z., and Svoboda, K. (2008). Sparse optical microstimulation in barrel cortex drives learned behaviour in freely moving mice. Nature *451*, 61–64.

Jia, H., Rochefort, N.L., Chen, X., and Konnerth, A. (2011). In vivo two-photon imaging of sensory-evoked dendritic calcium signals in cortical neurons. Nat. Protoc. *6*, 28–35.

Jones, H.E., Grieve, K.L., Wang, W., and Sillito, A.M. (2001). Surround suppression in primate V1. J. Neurophysiol. *86*, 2011–2028.

Keller, G.B., Bonhoeffer, T., and Hübener, M. (2012). Sensorimotor Mismatch Signals in Primary Visual Cortex of the Behaving Mouse. Neuron *74*, 809–815.

Kepecs, A., Uchida, N., Zariwala, H.A., and Mainen, Z.F. (2008). Neural correlates, computation and behavioural impact of decision confidence. Nature *455*, 227–231.

Kerlin, A.M., Andermann, M.L., Berezovskii, V.K., and Reid, R.C. (2010). Broadly Tuned Response Properties of Diverse Inhibitory Neuron Subtypes in Mouse Visual Cortex. Neuron *67*, 858–871.

Kilpeläinen, M., Nurminen, L., and Donner, K. (2011). Effects of Mean Luminance Changes on Human Contrast Perception: Contrast Dependence, Time-Course and Spatial Specificity. PLoS ONE *6*, e17200.

Lak, A., Schröder, S., Jacobs, E., Soares, S., Burgess, C.P., Paton, J.J., Harris, K.D., and Carandini, M. (2015). Midbrain dopamine stimulation enhances perceptual sensitivity. In Neuroscience 2015 Abstracts, (Chicago, IL),.

Leopold, D.A., and Logothetis, N.K. (1996). Activity changes in early visual cortex reflect monkeys' percepts during binocular rivalry. Nature *379*, 549–553.

Luo, L., Callaway, E.M., and Svoboda, K. (2008). Genetic Dissection of Neural Circuits. Neuron *57*, 634–660.

Madisen, L., Garner, A.R., Shimaoka, D., Chuong, A.S., Klapoetke, N.C., Li, L., van der Bourg, A., Niino, Y., Egolf, L., Monetti, C., et al. (2015). Transgenic Mice for Intersectional Targeting of Neural Sensors and Effectors with High Specificity and Performance. Neuron *85*, 942–958.

Mank, M., Santos, A.F., Direnberger, S., Mrsic-Flogel, T.D., Hofer, S.B., Stein, V., Hendel, T., Reiff, D.F., Levelt, C., Borst, A., et al. (2008). A genetically encoded calcium indicator for chronic in vivo two-photon imaging. Nat. Methods *5*, 805–811.

Marshel, J.H., Garrett, M.E., Nauhaus, I., and Callaway, E.M. (2011). Functional specialization of seven mouse visual cortical areas. Neuron *72*, 1040–1054.

Morin, L.P., and Studholme, K.M. (2014). Retinofugal projections in the mouse. J. Comp. Neurol. *522*, 3733–3753.

Mountcastle, V.B., Steinmetz, M.A., and Romo, R. (1990). Frequency discrimination in the sense of flutter: psychophysical measurements correlated with postcentral events in behaving monkeys. J. Neurosci. *10*, 3032–3044.

Newsome, W.T., Britten, K.H., and Movshon, J.A. (1989a). Neuronal correlates of a perceptual decision. Nature *341*, 52–54.

Newsome, W.T., Britten, K.H., and Movshon, J.A. (1989b). Neuronal correlates of a perceptual decision. Nature *341*, 52–54.

Niell, C.M., and Stryker, M.P. (2008). Highly Selective Receptive Fields in Mouse Visual Cortex. J. Neurosci. *28*, 7520–7536.

Nienborg, H., and Cumming, B.G. (2006). Macaque V2 Neurons, But Not V1 Neurons, Show Choice-Related Activity. J. Neurosci. *26*, 9567–9578.

Nienborg, H., and Cumming, B.G. (2009). Decision-related activity in sensory neurons reflects more than a neuron's causal effect. Nature *459*, 89–92.

Nienborg, H., and Cumming, B.G. (2014). Decision-Related Activity in Sensory Neurons May Depend on the Columnar Architecture of Cerebral Cortex. J. Neurosci. *34*, 3579–3585.

Okun, M., Carandini, M., and Harris, K.D. (2015). Long term recordings with immobile silicon probes in the mouse cortex. bioRxiv 021691.

Olds, J., and Milner, P. (1954). Positive reinforcement produced by electrical stimulation of septal area and other regions of rat brain. J. Comp. Physiol. Psychol. *47*, 419–427.

Otazu, G.H., Tai, L.-H., Yang, Y., and Zador, A.M. (2009). Engaging in an auditory task suppresses responses in auditory cortex. Nat. Neurosci. *12*, 646–654.

Palmer, C., Cheng, S.-Y., and Seidemann, E. (2007). Linking Neuronal and Behavioral Performance in a Reaction-Time Visual Detection Task. J. Neurosci. *27*, 8122–8137.

Pologruto, T.A., Sabatini, B.L., and Svoboda, K. (2003). ScanImage: Flexible software for operating laser scanning microscopes. Biomed. Eng. OnLine *2*, 13.

Poort, J., Khan, A.G., Pachitariu, M., Nemri, A., Orsolic, I., Krupic, J., Bauza, M., Sahani, M., Keller, G.B., Mrsic-Flogel, T.D., et al. (2015). Learning Enhances Sensory and Multiple Non-sensory Representations in Primary Visual Cortex. Neuron *86*, 1478–1490.

Posner, M.I., and Gilbert, C.D. (1999). Attention and primary visual cortex. Proc. Natl. Acad. Sci. U. S. A. *96*, 2585–2587.

Raz, A., and Buhle, J. (2006). Typologies of attentional networks. Nat. Rev. Neurosci. *7*, 367–379.

Ress, D., Backus, B.T., and Heeger, D.J. (2000). Activity in primary visual cortex predicts performance in a visual detection task. Nat. Neurosci. *3*, 940–945.

Resulaj, A., Kiani, R., Wolpert, D.M., and Shadlen, M.N. (2009). Changes of mind in decision-making. Nature *461*, 263–266.

Runyan, C.A., Schummers, J., Van Wart, A., Kuhlman, S.J., Wilson, N.R., Huang, Z.J., and Sur, M. (2010). Response Features of Parvalbumin-Expressing Interneurons Suggest Precise Roles for Subtypes of Inhibition in Visual Cortex. Neuron *67*, 847–857.

Sachidhanandam, S., Sreenivasan, V., Kyriakatos, A., Kremer, Y., and Petersen, C.C.H. (2013). Membrane potential correlates of sensory perception in mouse barrel cortex. Nat. Neurosci. *16*, 1671–1677.

Saleem, A.B., Ayaz, A., Jeffery, K.J., Harris, K.D., and Carandini, M. (2013). Integration of visual motion and locomotion in mouse visual cortex. Nat. Neurosci. *16*, 1864–1869.

Sanders, J.I., and Kepecs, A. (2012). Choice ball: a response interface for two-choice psychometric discrimination in head-fixed mice. J. Neurophysiol. *108*, 3416–3423.

Scherberger, H., and Andersen, R.A. (2007). Target Selection Signals for Arm Reaching in the Posterior Parietal Cortex. J. Neurosci. *27*, 2001–2012.

Steinmetz, N.A., Burgess, C.P., Rossant, C., Kadir, S.N., Goodman, D.F.M., Hunter, M.L.D., Carandini, M., and Harris, K.D. (2015). Neural correlates of visually--guided behavior in mouse cingulate cortex. In Neuroscience 2015 Abstracts, (Chicago, IL: Society for Neuroscience),.

Stüttgen, M.C., and Schwarz, C. (2008). Psychophysical and neurometric detection performance under stimulus uncertainty. Nat. Neurosci. *11*, 1091–1099.

Tolhurst, D.J., Movshon, J.A., and Dean, A.F. (1983). The statistical reliability of signals in single neurons in cat and monkey visual cortex. Vision Res. *23*, 775–785.

Van den Bergh, G., Zhang, B., Arckens, L., and Chino, Y.M. (2010). Receptive-field properties of V1 and V2 neurons in mice and macaque monkeys. J. Comp. Neurol. *518*, 2051–2070.

Vogels, R., and Orban, G.A. (1990). How well do response changes of striate neurons signal differences in orientation: a study in the discriminating monkey. J. Neurosci. *10*, 3543–3558.